

Diamine Bis(phenolate) as Supporting Ligands in Organoactinide(IV) Chemistry. Synthesis, Structural Characterization, and Reactivity of Stable Dialkyl Derivatives

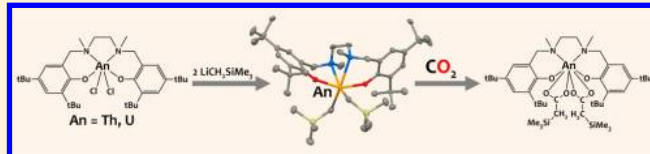
Elsa Mora,[†] Leonor Maria,^{*,†} Biplab Biswas,[‡] Clément Camp,[‡] Isabel C. Santos,[†] Jacques Pécaut,[‡] Adelaide Cruz,[†] José M. Carretas,[†] Joaquim Marçalo,[†] and Marinella Mazzanti^{*,‡}

[†]Unidade de Ciências Químicas e Radiofarmacêuticas, IST/ITN, Instituto Superior Técnico, Universidade Técnica de Lisboa, 2686-953 Sacavém, Portugal

[‡]Laboratoire de Reconnaissance Ionique et Chimie de Coordination, SCIB, UMR-E CEA/UJF-Grenoble 1, INAC, CEA-Grenoble, 38054 Grenoble Cedex 09, France

Supporting Information

ABSTRACT: The homoleptic compounds $[\text{U}(\text{salan-R}_2)_2]$ ($\text{R} = \text{Me}$ (**1**), ^tBu (**2**)) were prepared in high yield by salt-metathesis reactions between $\text{UI}_4(\text{L})_2$ ($\text{L} = \text{Et}_2\text{O}$, PhCN) and 2 equiv of $[\text{K}_2(\text{salan-R}_2)]$ in THF. In contrast, the reaction of the tetradentate ligands salan-R_2 with $\text{UI}_3(\text{THF})_4$ leads to disproportionation of the metal and to mixtures of U(IV) $[\text{U}(\text{salan-R}_2)_2]$ and $[\text{U}(\text{salan-R}_2)\text{I}_2]$ complexes, depending on the ligand to M ratio. The reaction of $\text{K}_2\text{salan-Me}_2$ ligand with U(IV) iodide and chloride salts always leads to mixtures of the homoleptic bis-ligand complex $[\text{U}(\text{salan-Me}_2)_2]$ and heteroleptic complexes $[\text{U}(\text{salan-Me}_2)\text{X}_2]$ in different organic solvents. The structure of the heteroleptic complex $[\text{U}(\text{salan-Me}_2)\text{I}_2(\text{CH}_3\text{CN})]$ (**4**) was determined by X-ray studies. Heteroleptic U(IV) and Th(IV) chloride complexes were obtained in good yield using the bulky $\text{salan-}^t\text{Bu}_2$ ligand. The new complexes $[\text{U}(\text{salan-}^t\text{Bu}_2)\text{Cl}_2(\text{bipy})]$ (**5**) and $[\text{Th}(\text{salan-}^t\text{Bu}_2)\text{Cl}_2(\text{bipy})]$ (**8**) were crystallographically characterized. The $\text{salan-}^t\text{Bu}_2$ halide complexes of U(IV) and Th(IV) revealed good precursors for the synthesis of stable dialkyl complexes. The six-coordinated alkyl complexes $[\text{Th}(\text{salan-}^t\text{Bu}_2)(\text{CH}_2\text{SiMe}_3)_2]$ (**9**) and $[\text{U}(\text{salan-}^t\text{Bu}_2)(\text{CH}_2\text{SiMe}_3)_2]$ (**10**) were prepared by addition of $\text{LiCH}_2\text{SiMe}_3$ to the chloride precursor in toluene, and their solution and solid-state structures (for **9**) were determined by NMR and X-ray studies. These complexes are stable for days at room temperature. Preliminary reactivity studies show that CO_2 inserts into the An-C bond to afford a mixture of carboxylate products. In the presence of traces of LiCl , crystals of the dimeric insertion product $[\text{Th}_2\text{Cl}(\text{salan-}^t\text{Bu}_2)_2(\mu\text{-}\eta^1\text{:}\eta^2\text{-O}_2\text{CCH}_2\text{SiMe}_3)_2(\mu\text{-}\eta^1\text{:}\eta^2\text{-O}_2\text{CCH}_2\text{SiMe}_3)]$ (**11**) were isolated. The structure shows that CO_2 insertion occurs in both alkyl groups and that the resulting carboxylate is easily displaced by a chloride anion.



INTRODUCTION

Due to the large coordination numbers of actinides and the possible participation of 5f electrons in bonding and reactivity, actinide complexes can promote unusual reactivity and perform as more effective catalysts in comparison to lanthanides and d-block metals.^{1–7}

In particular, alkyl complexes of actinides can act as versatile catalysts in many transformations or participate as intermediates in catalytic transformations.^{8–11}

The chemistry of alkyl complexes of An(IV) has been extensively investigated since the early 1970s using cyclopentadienyl as an effective supporting ligand.^{12–19} The insertion reactions of substrates into the actinide–carbon bond have a key role in actinide-promoted transformation and functionalization of organic molecules, and accordingly, insertion reactions are also well documented in actinide metallocene chemistry,^{15,20–24} although only very few insertion products have been crystallographically characterized.

Previous studies show that the geometry and electronic properties of the ancillary ligand play an important role in the

reactivity and catalytic efficiency of organoactinide complexes.^{13,25,26}

However, only a few non-cyclopentadienyl supporting ligands have been used to prepare stable An(IV) alkyl complexes and to investigate their chemistry,^{27–29} which includes three dianionic ancillary ligands.^{30–35} Some of these systems have demonstrated high stability,³⁴ unprecedented reactivity such as C–C coupling³⁶ and C–H activation,³⁷ and catalytic activity in alkene polymerization or hydroamination.^{38–40} The use of non-cyclopentadienyl ligands has also recently led to the characterization of a rare monoalkyl U(III) species that can insert CO_2 and CS_2 into An-C bonds to yield the corresponding carboxylate and dithiocarboxylate complexes.⁴¹ These results highlight the interest in identifying

Special Issue: Recent Advances in Organo-f-Element Chemistry

Received: November 9, 2012

Published: December 18, 2012



new supporting ligands capable of stabilizing An alkyl complexes and in tuning their reactivity.

salans are tetradentate dianionic diamine bis(phenolate) ligands which are being increasingly used as supporting ligands in coordination chemistry and catalytic transformations promoted by transition metals^{42,43} and lanthanides.⁴⁴ Tetradentate salan ligands should provide a robust coordination environment for reactivity studies on uranium alkyl complexes and are good candidates for the development of uranium-based catalysts. Moreover, the bulk and electronic properties of these ligands can be easily tuned to optimize the stability and reactivity of the final complex. However, in uranium chemistry they have only been used to prepare stable uranyl(V) complexes and their uranyl(VI) analogues.^{45–47} Here we have investigated the ability of the tetradentate ligands $\text{salan-}^t\text{Bu}_2^{2-}$ ($\text{H}_2\text{salan-}^t\text{Bu}_2 = N,N'$ -bis(2-hydroxybenzyl-3,5-di-*tert*-butyl)-1,2-dimethylaminomethane) and salan-Me_2^{2-} ($\text{H}_2\text{salan-Me}_2 = N,N'$ -bis(2-hydroxybenzyl-3,5-methyl)-1,2-dimethylaminomethane) to form complexes with uranium in lower oxidation states. We show that the bulky $\text{salan-}^t\text{Bu}_2^{2-}$ ligand provides a suitable environment for the synthesis of heteroleptic An(IV) halide complexes, $[\text{An}(\text{salan-}^t\text{Bu}_2)\text{X}_2]$, which provide versatile precursors for the synthesis of robust alkyl complexes. The reaction of CO_2 insertion with these alkyl complexes is also described.

EXPERIMENTAL SECTION

General Considerations. All air- and moisture-sensitive manipulations were performed using standard Schlenk techniques or in an inert-atmosphere glovebox filled with nitrogen or argon. Tetrahydrofuran, dimethoxyethane, toluene, and *n*-hexane were predried using 4A molecular sieves, distilled under nitrogen from sodium-benzophenone, and degassed prior to use. Tetrahydrofuran- d_8 , benzene- d_6 , and toluene- d_8 were dried over sodium-benzophenone and distilled under argon. Acetonitrile and acetonitrile- d_3 were distilled from P_2O_5 or CaH_2 under argon and maintained in contact with 3A molecular sieves several days before use.

$\text{UCl}_3(\text{THF})_4$, UCl_4 , $\text{U}(\text{L})_n$ ($\text{L} = \text{Et}_2\text{O}$, PhCN), and $\text{ThCl}_4(\text{dme})_2$ were prepared using previously reported procedures.^{48–52} The dianionic salan-R_2 ligand precursors and the potassium salts were synthesized as previously reported.⁵³ 2,2'-Bipyridine was sublimed before use. Pentane was removed under vacuum from $\text{LiCH}_2\text{Si}(\text{CH}_3)_3$ (1.0 M, Aldrich) prior to use.

The NMR experiments (^1H , ^{13}C , COSY, HSQC) were performed on Varian 300 and 400 MHz and Bruker 200 MHz spectrometers; all chemical shifts are reported relative to the peak for SiMe_4 using ^1H and ^{13}C chemical shifts of residual solvents. CHN elemental analyses were performed using a CE Instruments EA1110 automatic analyzer or by Analytische Laboratorien GMBH at Lindlar, Germany. Electrospray ionization mass spectrometry (ESI/MS) was performed using a Bruker HCT quadrupole ion trap equipped with an electrospray interface; the samples were prepared under N_2 with dry solvents, and the airtight syringe was filled inside an inert-atmosphere glovebox and carried in a closed vessel under N_2 before injection.

Synthesis of $[\text{U}(\text{salan-Me}_2)_2]$ (1). *Method 1.* A green solution of $\text{UCl}_3(\text{THF})_4$ (49 mg, 0.054 mmol, 1 equiv) in acetonitrile (1 mL) was added to a suspension of $[\text{K}_2(\text{salan-Me}_2)]$ (23.3 mg, 0.0540 mmol, 1 equiv) in acetonitrile (1 mL). The resulting suspension was stirred for 30 min, and the solids were removed by filtration. The resulting green solution was left to stand at room temperature for 1 day to yield X-ray-quality crystals of **1** in 55% yield (15 mg, 0.015 mmol).

Method 2. A brown solution of $\text{U}(\text{L})(\text{Et}_2\text{O})_2$ (50 mg, 0.056 mmol) in 1.5 mL of THF was added to a suspension of $[\text{K}_2(\text{salan-Me}_2)]$ (48.3 mg, 0.111 mmol) in THF (1.5 mL). The resulting mixture was stirred for 0.5 h, at room temperature, until the suspension became green. The white solid that formed was removed by filtration, and the solution was concentrated and left standing at room temperature for

few days. Complex **1** was obtained as a green microcrystalline solid in 73% yield (39 mg, 0.041 mmol). Anal. Calcd for $\text{C}_{44}\text{H}_{60}\text{N}_4\text{O}_4\text{U}$: C, 55.80; H, 6.38; N, 5.91. Found: C, 55.48; H, 6.28; N, 5.88. ^1H NMR (200 MHz, $\text{THF-}d_8$, 298 K): δ 41.2 (s, 4H), 15.5 (s, 12H), 12.6 (s, 4H), 7.4 (s, 4H), 3.2 (s, 12H), -4.3 (s, 4H), -12.0 (s, 12H), -33.2 (s, 4H), -52.4 (s, 4H).

Synthesis of $[\text{U}(\text{salan-}^t\text{Bu}_2)_2]$ (2). *Method 1.* A green solution of $\text{UCl}_3(\text{THF})_4$ (50 mg, 0.055 mmol) in 1 mL of acetonitrile was added to a suspension of $[\text{K}_2(\text{salan-}^t\text{Bu}_2)]$ (33 mg, 0.055 mmol) in acetonitrile (1 mL). The resulting mixture was stirred for 1 h at room temperature. The KI that formed was removed by filtration, and the resulting brown solution was transferred to a crystallization tube. After 2 days at room temperature, green crystals suitable for X-ray diffraction of compound **2**·1.25 CH_3CN were obtained. Yield: 65% (23 mg, 0.018 mmol). Crystals of **2**·THF of better quality were obtained from a THF solution. Anal. Calcd for $\text{C}_{68}\text{H}_{108}\text{N}_4\text{O}_4\text{U}\cdot\text{CH}_3\text{CN}$: C, 63.47; H, 8.45; N, 5.29. Found: C, 63.21; H, 8.59; N, 5.40.

Method 2. Complex **2** can also be obtained from the addition of a brown solution of $\text{U}(\text{L})(\text{Et}_2\text{O})_2$ (37 mg, 0.042 mmol) in 1 mL of THF to a suspension of $[\text{K}_2(\text{salan-}^t\text{Bu}_2)]$ (50 mg, 0.083 mmol) in THF (1.5 mL). The resulting suspension was stirred for 3 h at room temperature and then filtered to afford the final compound. Yield: 78% (42 mg, 0.033 mmol). Crystals of **2**·THF were grown from a tetrahydrofuran solution at room temperature and confirmed the presence of the bis-ligand complex. The ^1H NMR of **2** in THF at room temperature displays a series of broad signals. ^1H NMR (400 MHz, $\text{THF-}d_8$, 233 K): 80.99 (s, 2H), 53.55 (s, 6H, NCH_3), 31.51 (s, 18H, $\text{C}(\text{CH}_3)_3$), 30.99 (s, 2H), 12.88 (s, 2H), 6.99 (s, 18H, $\text{C}(\text{CH}_3)_3$), -1.51 (s, 18H, $\text{C}(\text{CH}_3)_3$), -2.24 (s, 2H), -2.92 (s, 2H), -5.74 (s, 18H, $\text{C}(\text{CH}_3)_3$), -7.53 (s, 2H), -10.49 (s, 2H), -26.81 (s, 2H), -38.54 (s, 2H), -43.59 (s, 2H), -57.32 (s, 2H), -59.09 (s, 6H, $\text{C}(\text{CH}_3)_3$), -72.52 (s, 2H). ^1H NMR (300 MHz, C_7D_8 , 233 K): 78.95 (s, 2H), 51.19 (s, 6H, NCH_3), 30.89 (s, 18H, $\text{C}(\text{CH}_3)_3$), 12.64 (s, 2H), 8.60 (s, 2H), 6.82 (s, 18H, $\text{C}(\text{CH}_3)_3$), -1.14 (s, 18H, $\text{C}(\text{CH}_3)_3$), -1.50 (s, 2H), -2.85 (s, 2H), -5.32 (s, 18H, $\text{C}(\text{CH}_3)_3$), -7.02 (s, 2H), -9.68 (s, 2H), -26.00 (s, 2H), -38.45 (s, 2H), -42.99 (s, 2H), -55.79 (s, 2H), -56.82 (s, 6H, NCH_3), -70.24 (s, 2H).

Isolation of Crystals of $[\text{U}(\text{salan-}^t\text{Bu}_2)_2(\text{bipy})]$ (3). To a solution of $\text{UCl}_3(\text{THF})_4$ (332 mg, 0.38 mmol) in THF (10 mL) was added a solution of $[\text{K}_2(\text{salan-}^t\text{Bu}_2)]$ (228 mg, 0.38 mmol) in THF (10 mL), and the mixture was stirred at room temperature for 2 h. A solution of 2,2'-bipyridine (60 mg, 0.38 mmol) in THF (0.5 mL) was then added, and the mixture was stirred overnight at room temperature. After centrifugation, the solvent was removed under vacuum, giving a dark green solid, which was further extracted with toluene. Green crystals adequate for X-ray diffraction analysis were obtained by slow diffusion of *n*-hexane into a concentrated toluene solution of the mixture. ^1H NMR (300 MHz, C_6D_6 , 298 K): 169.90 (2H, br), 48.26 (18H, s, $\text{C}(\text{CH}_3)_3$), 43.50 (2H, s), 22.03 (2H, s), 17.13 (2H, s), 10.34 (18H, s, $\text{C}(\text{CH}_3)_3$), 3.30 (2H, s), -22.03 (2H, s), -30.31 (2H, br), -44.79 (2H, br), -50.16 (2H + 2H, s), -63.85 (6H, s, NCH_3).

This complex could not be obtained analytically pure in large quantity because the formation of **3** is always accompanied by the presence of $[\text{U}(\text{salan-}^t\text{Bu}_2)_2]$ (**2**).

Isolation of Crystals of $[\text{U}(\text{salan-Me}_2)_2(\text{CH}_3\text{CN})]$ (4). A brown solution of $\text{U}(\text{L})(\text{PhCN})_4$ (50 mg, 0.043 mmol, 1 equiv) in acetonitrile (1.5 mL) was added to a suspension of $[\text{K}_2(\text{salan-Me}_2)]$ (18.7 mg, 0.043 mmol, 1 equiv) in acetonitrile (1.5 mL). The resulting suspension was stirred for 3 h until it became green, and then the white precipitate of KI was removed by filtration. The resulting green solution was transferred to a crystallization tube, and after 3 days X-ray-quality crystals of **4** were formed. ^1H NMR (200 MHz, $\text{THF-}d_8$, 298 K): δ 81.4 (s, 6H), 47.6 (s, 2H), 20.6 (s, 2H), 19.8 (s, 6H), -26.0 (s, 2H), -33.0 (s, 2H), -53.5 (s, 4H), -76.4 (s, 6H).

This complex could not be obtained analytically pure in large quantity because the formation of **4** is always accompanied by the presence of $[\text{U}(\text{salan-Me}_2)_2]$ (**1**). Although complex **4** is more insoluble, it was impossible to obtain an analytically pure complex by crystallization.

Synthesis of [U(salan-¹Bu₂)Cl₂(bipy)] (5). To a green solution of UCl₄ (289 mg, 0.76 mmol) in THF (10 mL) was slowly added a solution of [K₂(salan-¹Bu₂)] (457 mg, 0.76 mmol) in THF (15 mL), and the mixture was stirred for 30 min to afford the mono-ligand complex [U(salan-¹Bu₂)Cl₂(THF)_x] (¹H NMR (200 MHz, THF-*d*₈, 298 K): δ 52.6 (s, 18H, C(CH₃)₃), 47.3 (s, 2H), 20.4 (s, 2H), 11.5 (s, 18H, C(CH₃)₃), -23.9 (s, 2H), -33.6 (s, 2H), -52.2 (s, 2H), -53.3 (s, 2H), -76.9 (s, 6H, NCH₃). Then it was added to a solution of 2,2'-bipyridine (119 mg, 0.76 mmol) in THF (0.5 mL). After the reaction mixture was stirred overnight at room temperature, the potassium chloride was separated by centrifugation and the solvent was removed under vacuum. After the residue was washed three times with 2 mL of acetonitrile and once with 3 mL of *n*-hexane and dried under vacuum, a green solid was obtained and identified as **5** (459 mg, 0.464 mmol, 61%). Green crystals of **5** suitable for X-ray diffraction analysis were obtained by slow diffusion of *n*-hexane into a saturated toluene solution. Anal. Calcd for C₄₄H₆₂N₄O₂Cl₂U: C, 53.49; H, 6.33; N, 5.67. Found: C, 53.75; H, 6.70; N, 5.80. MS (ESI/MS, CH₃CN/THF): *m/z* 853.4 [U(salan-¹Bu₂)Cl₂Na]⁺, 869.5 [U(salan-¹Bu₂)Cl₂K]⁺, 951.4 [U(salan-¹Bu₂)Cl(bipy)]⁺, 867.4 [U(salan-¹Bu₂)Cl₃]⁻. ¹H NMR (300 MHz, C₆D₆, 298 K): δ 154.39 (2H, br), 45.90 (s, 18H, C(CH₃)₃), 41.96 (s, 2H), 24.14 (s, 2H), 19.07 (s, 2H), 17.51 (s, 2H), 17.17 (s, 2H), 10.15 (s, 18H, C(CH₃)₃), -24.08 (s, 2H), -27.20 (s, 2H), -38.79 (br, 2H), -48.91 (s, 2H+2H), -64.80 (s, 6H, NCH₃).

Isolation of Crystals of [Th(salan-¹Bu₂)₂] (6). To a suspension of ThCl₄(dme)₂ (158 mg, 0.285 mmol, 1 equiv) in tetrahydrofuran (10 mL) was added a solution of [K₂(salan-¹Bu₂)] (344 mg, 0.572 mmol, 2 equiv) in THF (5 mL). The resulting suspension was stirred overnight at room temperature, and then the white precipitate of KCl was removed by centrifugation. Evaporation under reduced pressure produced a white solid. Complex **6** could not be obtained analytically pure because the formation of **6** is always accompanied by the presence of [Th(salan-¹Bu₂)Cl₂] and other species, and separation of **6** by crystallization proved to be difficult. A few crystals adequate for X-ray diffraction analysis were grown from a saturated hexane solution. ¹H NMR (300 MHz, C₆D₆, 298 K): δ 7.61 (d, 4H, Ar-H), 6.73 (d, *J*_{HH} = 2.7 Hz, 4H, Ar-H), 5.85 (d, *J*_{HH} = 12.7 Hz, 4H, ArCH₂N), 3.11 (d, *J*_{HH} = 9 Hz, 4H, NCH₂CH₂N), 2.82 (d, *J*_{HH} = 4H, 12.96 Hz, ArCH₂N), 2.67 (s, 6H, NCH₃), 1.82 (s, 36H, C(CH₃)₃), 1.27 (d, 4H, NCH₂CH₂N), 1.18 (s, 36H, C(CH₃)₃).

Synthesis of [Th(salan-¹Bu₂)Cl₂(dme)] (7). A solution of [K₂(salan-¹Bu₂)] (560 mg, 0.932 mmol) in 1,2-dimethoxyethane (10 mL) was added dropwise to a solution of ThCl₄(dme)₂ (516 mg, 0.932 mmol) in 1,2-dimethoxyethane (10 mL), and the mixture was stirred overnight at room temperature. The mixture was centrifuged, and the volatiles were removed under reduced pressure. The residue was extracted with a mixture of 10 mL of toluene and 0.4 mL of dme, and the resulting solution was concentrated under vacuum. A white microcrystalline solid was isolated by centrifugation, washed with *n*-hexane, and dried under vacuum to give **7** (632 mg, 0.690 mmol, 74%). Anal. Calcd for C₃₈H₆₄Cl₂N₂O₄Th·0.2(toluene): C, 50.65; H, 7.08; N, 3.30. Found: C, 50.77; H, 7.44; N, 3.08. MS (ESI/MS, CH₃CN): *m/z* 863.2 [Th(salan-¹Bu₂)Cl₂K]⁺, 861.4 [Th(salan-¹Bu₂)Cl₃]⁻. ¹H NMR (300 MHz, C₆D₆, 298 K): δ 7.68 (2H, d, *J*_{HH} = 2.5 Hz, Ar), 6.92 (2H, d, *J*_{HH} = 2.5 Hz, Ar), 5.29 (2H, d, *J*_{HH} = 13.8 Hz, ArCH₂N), 2.78 (2H, d, *J*_{HH} = 13.8 Hz, ArCH₂N), 3.78 (br, OCH₂CH₂O), 3.31 (br, OCH₃), 2.99 (2H, d, *J*_{HH} = 10.4 Hz, NCH₂CH₂N), 2.55 (6H, s, NCH₃), 1.82 (18H, s, C(CH₃)₃), 1.34 (18H, s, C(CH₃)₃), 1.20 (2H, d, *J*_{HH} = 10.4 Hz, NCH₂CH₂N). ¹³C NMR (75.4 MHz, C₆D₆, 298 K): δ 159.6 (Ar-C-O), 140.6 (Ar-C), 137.2 (Ar-C), 126.7 (Ar-C), 125.7 (Ar-CH), 125.1 (Ar-CH), 72.1 (OCH₂CH₂O), 64.5 (ArCH₂N), 63.1 (CH₃OCH₂CH₂OCH₃), 53.1 (NCH₂CH₂N), 47.8 (NCH₃), 34.6 (C(CH₃)₃), 34.4 (C(CH₃)₃), 31.9 (C(CH₃)₃), 31.5 (C(CH₃)₃). ¹H NMR (300 MHz, C₇D₈, 263 K): δ 7.66 (2H, d, *J* = 2.4 Hz, Ar), 6.91 (2H, d, *J* = 2.4 Hz, Ar), 5.24 (2H, d, *J* = 13.5 Hz, ArCH₂N), 3.76 (2H, d, *J* = 6.9 Hz, OCH₂CH₂O), 3.30 (6H, s, CH₃O), 2.99 (2H, d, *J* = 9.9 Hz, NCH₂CH₂N), 2.77 (2H, d, 13.8 Hz, ArCH₂N), 2.65 (2H, d, *J* = 6.9 Hz, OCH₂CH₂O), 2.52 (6H, s, CH₃N), 1.81 (18H, s, C(CH₃)₃), 1.35 (18H, s, C(CH₃)₃), 1.20 (2H, d, *J* = 10.2, NCH₂CH₂N). ¹³C NMR (75.4 MHz, C₇D₈, 263 K): δ 159.5 (Ar-CO),

140.3 (Ar-C), 136.9 (Ar-C), 126.5 (Ar-C), 125.6 (Ar-CH), 71.9 (OCH₂CH₂O), 64.4 (ArCH₂N), 63.0 (CH₃O), 53.0 (NCH₂CH₂N), 47.7 (NCH₃), 35.5 (C(CH₃)₃), 34.3 (C(CH₃)₃), 31.9 (C(CH₃)₃), 31.2 (C(CH₃)₃).

Synthesis of [Th(salan-¹Bu₂)Cl₂(bipy)] (8). A 2,2'-bipyridine (34 mg, 0.22 mmol) toluene solution (1 mL) was added to a solution of **7** (200 mg, 0.22 mmol) in toluene (10 mL). After 1 h of stirring at room temperature the volatiles were removed under vacuum. The residue solid was redissolved in 4 mL of toluene, and addition of 8 mL of *n*-hexane afforded a white crystalline solid formulated as [Th(salan-¹Bu₂)Cl₂(bipy)] (170 mg, 0.173 mmol, 79%). X-ray-quality crystals were obtained by slow diffusion of *n*-hexane into a toluene solution of **8**. Anal. Calcd for C₄₄H₆₂Cl₂N₄O₂Th: C, 53.82; H, 6.36; N, 5.71. Found: C, 53.41; H, 6.25; N, 5.45. MS (ESI/MS, CH₃CN): *m/z* 863.5 [Th(salan-¹Bu₂)Cl₂K]⁺, 945.6 [Th(salan-¹Bu₂)Cl(bipy)]⁺, 861.5 [Th(salan-¹Bu₂)Cl₃]⁻. ¹H NMR (300 MHz, C₆D₆, 298 K): δ 9.17 (2H, d, 5.1 Hz, bipy), 7.78 (2H, d, *J*_{HH} = 2.4 Hz, Ar-H), 7.05 (2H, d, *J*_{HH} = 2.4 Hz, Ar-H), 6.92 (2H, d, 7.8 Hz, bipy), 6.85 (2H, m, bipy), 6.35 (2H, m, bipy), 5.56 (2H, d, *J*_{HH} = 13.7 Hz, ArCH₂N), 3.18 (2H, d, *J*_{HH} = 9.9 Hz, NCH₂CH₂N), 2.93 (2H, d, *J*_{HH} = 13.9 Hz, ArCH₂N), 2.69 (6H, s, CH₃), 1.78 (18H, s, C(CH₃)₃), 1.38 (18H, s, C(CH₃)₃), 1.33 (2H, d, *J*_{HH} = 9.07 Hz, NCH₂CH₂N). ¹³C NMR (75.4 MHz, C₆D₆, 298 K): δ 159.9 (Ar-CO), 154.8 (bipy-C), 152.3 (bipy-CH), 140.4 (Ar-C), 138.2 (bipy-CH), 137.6 (Ar-C), 127.2 (Ar-C), 126.1 (Ar-CH), 125.7 (Ar-C), 125.3 (Ar-CH), 123.8 (bipy-CH), 122.0 (bipy-CH), 64.6 (ArCH₂N), 53.1 (NCH₂CH₂N), 47.8 (NCH₃), 35.9 (C(CH₃)₃), 34.4 (C(CH₃)₃), 32.1 (C(CH₃)₃), 32.0 (C(CH₃)₃).

Synthesis of [Th(salan-¹Bu₂)(CH₂SiMe₃)₂] (9). To a solution of **7** (312 mg, 0.342 mmol) in toluene (10 mL) was added a solution of LiCH₂SiMe₃ (65 mg, 0.69 mmol) in toluene (1 mL). After 1 h of stirring at room temperature the resulting mixture was centrifuged and the solids were discarded. The volatiles were removed under reduced pressure, and the residue was washed with ca. 0.4 mL of *n*-hexane. The resulting white solid was redissolved in 3 mL of a 1/1 toluene/*n*-hexane mixture. Concentration of the solution led to the formation of white crystals of **9** suitable for X-ray diffraction analysis (210 mg, 0.226 mmol, 66%). Anal. Calcd for C₄₂H₇₆N₂O₂Si₂Th: C, 54.28; H, 8.24; N, 3.01. Found: C, 54.33; H, 8.31; N, 3.08. ¹H NMR (300 MHz, C₆D₆, 298 K): δ 7.62 (d, *J*_{HH} = 2.4 Hz, 2H, Ar-H), 6.86 (d, *J*_{HH} = 2.4 Hz, 2H, Ar-H), 4.13 (d, *J*_{HH} = 13.2 Hz, 2H, ArCH₂N), 2.66 (d, *J*_{HH} = 9.3 Hz, 2H, NCH₂CH₂N), 2.56 (d, *J*_{HH} = 13.2 Hz, 2H, ArCH₂N), 1.75 (s, 18H, C(CH₃)₃), 1.69 (s, 6H, NCH₃), 1.31 (s, 18H, C(CH₃)₃), 1.05 (d, *J*_{HH} = 9.3 Hz, 2H, NCH₂CH₂N), 0.36 (s, 18H, Si(CH₃)₃), 0.30 (d, *J*_{HH} = 10.2 Hz, 2H, Th-CH₂), 0.00 (d, *J*_{HH} = 10.2 Hz, 2H, Th-CH₂). ¹³C NMR (75.4 MHz, C₆D₆, 298 K): δ 161.0 (Ar-CO), 140.6 (Ar-C), 136.9 (Ar-C), 125.6 (Ar-C), 125.0 (Ar-CH), 124.8 (Ar-CH), 87.2 (CH₂SiMe₃), 63.0 (ArCH₂N), 51.3 (NCH₂CH₂N), 42.1 (NCH₃), 35.5 (C(CH₃)₃), 34.4 (C(CH₃)₃), 31.9 (C(CH₃)₃), 31.4 (C(CH₃)₃), 4.21 (Si(CH₃)₃).

Synthesis of [U(salan-¹Bu₂)(CH₂SiMe₃)₂] (10). To a solution of UCl₄ (217 mg, 0.57 mmol) in THF (10 mL) was added a solution of [K₂(salan-¹Bu₂)] (344 mg, 0.57 mmol) in THF (10 mL), and the mixture was stirred overnight at room temperature. The resulting mixture was centrifuged, and the solvent was removed under reduced pressure to give [U(salan-¹Bu₂)Cl₂(THF)_x]. Toluene was added to the solid residue, and to the resulting suspension was added a solution of LiCH₂SiMe₃ (108 mg, 1.14 mmol) in toluene (1 mL). The mixture was stirred for 1 h at room temperature and centrifuged, and the LiCl that formed was discarded. The volatiles were removed under reduced pressure, giving a dark green solid, which was further extracted with *n*-hexane. The first crop of the hexane solution (0.5 mL) was discarded, and the following crops were evaporated under reduced pressure, giving compound **10** as a green solid (247 mg, 0.264 mmol, 46%). An analytically pure sample was obtained from concentration of a saturated THF solution. Anal. Calcd for C₄₂H₇₆N₂O₂Si₂U: C, 53.94; H, 8.19; N, 3.00. Found: C, 53.64; H, 8.62; N, 2.91. ¹H NMR (300 MHz, C₆D₆, 298 K, ppm): δ 46.621 (s, 18H, C(CH₃)₃), 42.67 (s, 2H), 19.21 (s, 2H), 10.46 (s, 18H, C(CH₃)₃), -10.894–10. (s, 18H, Si(CH₃)₃), -17.68 (s, 2H), -26.55 (s, 2H), -47.41 (s, 2H), -50.90

Table 1. X-ray Crystal Data and Collection Parameters for the Uranium Complexes

	2·1.25CH ₃ CN	2·C ₄ H ₈ O	3·2C ₇ H ₈	4	5·C ₇ H ₈
empirical formula	C _{70.50} H _{111.75} N _{5.25} O ₄ U	C ₇₂ H ₁₁₆ N ₄ O ₃ U	C ₅₈ H ₇₈ I ₂ N ₄ O ₂ U	C ₂₄ H ₃₃ I ₂ N ₃ O ₂ U	C ₅₁ H ₆₇ Cl ₂ N ₄ O ₂ U
fw	1334.93	1355.72	1355.07	887.36	1077.02
temp (K)	150(2)	150(2)	150(2)	150(2)	150(2)
cryst syst	triclinic	monoclinic	monoclinic	tetragonal	monoclinic
space group	<i>P</i> $\bar{1}$	<i>C</i> 2/ <i>c</i>	<i>P</i> 2 ₁ / <i>c</i>	<i>P</i> 4 ₃ 2 ₁ 2	<i>C</i> 2/ <i>c</i>
<i>a</i> (Å)	15.1010(4)	18.2767(3)	10.1592(9)	8.52423(14)	34.0855(8)
<i>b</i> (Å)	15.3382(5)	24.4463(4)	31.130(3)	8.52423(14)	16.1899(3)
<i>c</i> (Å)	36.8413(6)	16.6782(3)	18.5587(17)	38.5227(12)	18.7980(4)
α (deg)	85.198(2)	90	90	90	90
β (deg)	78.323(2)	99.620(1)	91.005(3)	90	105.919(2)
γ (deg)	60.699(3)	90	90	90	90
<i>V</i> (Å ³)	7286.3(4)	7347.0(2)	5868.4(10)	2799.15(11)	9975.7(4)
<i>Z</i>	4	4	4	4	8
ρ_{calcd} (Mg/m ³)	1.217	1.226	1.534	2.106	1.434
μ (mm ^{−1})	2.273	2.256	3.859	8.028	3.402
R1 ^a (<i>I</i> > 2 σ (<i>I</i>))	0.0635	0.0309	0.0719	0.0439	0.0363
wR2 ^a (all data)	0.1459	0.0838	0.1571	0.0845	0.0900

^aDefinitions: R1 = $\sum ||F_o| - |F_c|| / \sum |F_o|$; wR2 = $[\sum w(F_o^2 - F_c^2)^2 / \sum w(F_o^2)^2]^{1/2}$.

Table 2. X-ray Crystal Data and Collection Parameters for the Thorium Complexes

	6·C ₆ H ₁₄	8·3C ₇ H ₈	9	11·4C ₇ H ₈
empirical formula	C ₇₄ H ₁₂₂ N ₄ O ₄ Th	C ₁₀₉ H ₁₄₈ Cl ₄ N ₈ O ₄ Th ₂	C ₄₂ H ₇₆ N ₂ O ₂ Si ₂ Th	C ₁₁₁ H ₁₇₃ ClN ₄ O ₁₀ Si ₃ Th ₂
fw	1363.80	2240.23	929.27	2307.33
temp (K)	150(2)	150(2)	150(2)	150(2)
cryst syst	monoclinic	trigonal	monoclinic	triclinic
space group	<i>C</i> 2/ <i>c</i>	<i>R</i> $\bar{3}$	<i>C</i> 2/ <i>c</i>	<i>P</i> $\bar{1}$
<i>a</i> (Å)	18.2062(4)	41.4321(13)	20.0165(4)	18.1779(3)
<i>b</i> (Å)	24.5461(4)	41.4321(13)	10.3489(2)	18.2607(3)
<i>c</i> (Å)	16.5539(3)	19.3575(7)	21.9123(5)	20.3703(4)
α (deg)	90	90	90	109.6670(10)
β (deg)	98.9980(10)	90	92.1110(10)	97.926(2)
γ (deg)	90	120	90	108.813(2)
<i>V</i> (Å ³)	7306.8(2)	28777.5(16)	4536.03(16)	5792.2(2)
<i>Z</i>	4	9	4	2
ρ_{calcd} (Mg/m ³)	1.240	1.163	1.361	1.323
μ (mm ^{−1})	2.088	2.450	3.373	2.672
R1 ^a (<i>I</i> > 2 σ (<i>I</i>))	0.0247	0.0364	0.0252	0.0414
wR2 ^a (all data)	0.0524	0.0792	0.0501	0.1056

^aDefinitions: R1 = $\sum ||F_o| - |F_c|| / \sum |F_o|$; wR2 = $[\sum w(F_o^2 - F_c^2)^2 / \sum w(F_o^2)^2]^{1/2}$.

(s, 2H), −86.19 (s, 6H, NCH₃), −236.43 (s, 2H, CH₂SiMe₃), −238.53 (s, 2H, CH₂SiMe₃).

Isolation of [Th₂Cl(salan-^tBu)₂(μ - η^1 : η^1 -O₂CCH₂SiMe₃)₂(μ - η^1 : η^2 -O₂CCH₂SiMe₃)] (11). A Schlenk tube was charged with **9** (98 mg, 0.106 mmol) and toluene (5 mL). The solution was degassed by three freeze–pump–thaw cycles, and CO₂ (2.3 mmol) was expanded into the tube (1 atm). The reaction mixture was stirred for 1 h at room temperature, and then the solvent was removed under vacuum. The white solid obtained was analyzed by ¹H NMR and ESI/MS, showing that a mixture of compounds was formed. A few crystals of **11** were isolated by slow evaporation of a toluene solution of the bulk product. Attempts to synthesize complex **11** in analytically pure form have failed, which is consistent with the NMR and ESI/MS analysis. Even in the presence of an excess of LiCl the ESI/MS and NMR analysis shows the presence of a mixture of compounds. In the presence of excess LiCl, the mono-chloride [Th(salan-^tBu)(O₂CCH₂SiMe₃)₂Cl][−] and bis-chloride [Th(salan-^tBu)(O₂CCH₂SiMe₃)₂Cl₂][−] species are both present in solution. The neutral bis-carboxylate is also present in solution, even in the presence of excess chloride. The presence of multiple species and of excess LiCl renders difficult the synthesis and characterization of **11**.

NMR Tube Scale Reaction of [An(salan-^tBu)₂(CH₂SiMe₃)₂] (An = Th (9**), U (**10**)) with CO₂.** A 10–30 mg portion of the bis(alkyl) actinide was dissolved in C₇D₈ (0.4 mL), and the solution was freeze–pump–thawed three times. The solution was then exposed to 1 atm of CO₂ (2 equiv or excess) at room temperature. The reaction was monitored by ¹H NMR spectroscopy and ESI/MS.

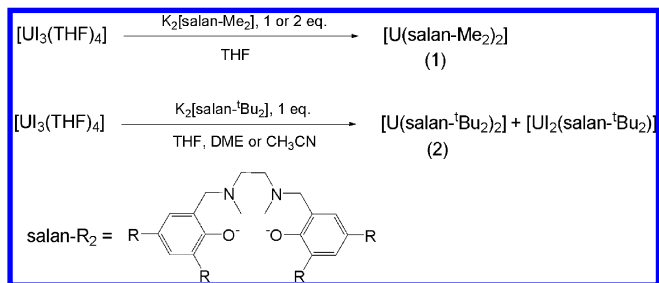
X-ray Crystallography. Crystallographic and experimental details of data collection and crystal structure refinement are summarized in Tables 1 and 2. Suitable crystals of complexes were selected and coated in FOMBLIN oil under an inert atmosphere. Crystals were then mounted on a loop, and the data were collected using graphite-monochromated Mo K α (λ = 0.71073 Å) on a Bruker AXS-KAPPA APEX II area detector or an Oxford Diffraction X-Calibur S diffractometer equipped with an Oxford Cryosystem open-flow nitrogen cryostat, and data were collected at 150 K. Cell parameters were retrieved using Bruker SMART or CrysAlisPro CCD software and refined using Bruker SAINT or CrysAlisPro Red on all observed reflections. Absorption corrections were applied using SADABS or ABSPACK.⁵⁴ The structures were solved by direct methods using either SHELXS-97⁵⁵ or SIR 97⁵⁶ or SHELXTL 6.10 and refined using full-matrix least-squares refinement against *F*² using SHELXL-97.⁵⁵ In

the former case, all programs are included in the package of programs WINGX-version 1.64.05.⁵⁷ All non-hydrogen atoms were refined anisotropically, unless it was mentioned in the cif files of the structures, and all hydrogen atoms were placed in idealized positions and allowed to refine riding on the parent carbon atom.

RESULTS AND DISCUSSION

Reactivity of U(III) with salan-R₂. The reaction of UI₃(THF)₄ with 1 equiv of [K₂(salan-Me₂)] in CH₃CN led to the isolation of the homoleptic uranium(IV) complex [U(salan-Me₂)₂] (1) (Scheme 1). Proton NMR spectra of 1/1

Scheme 1. Reaction of [UI₃(THF)₄] with salan-R₂ Ligands (R = Me, ^tBu)



and 1/2 reaction mixtures of UI₃(THF)₄ and K₂(salan-Me₂) show the presence of only one set of signals assigned to complex 1. X-ray diffraction studies on crystals isolated from both solutions confirmed the presence of the bis-ligand complex. While the crystals were not of sufficient quality to discuss the metrical parameters, the connectivity clearly shows the presence of a bis-ligand complex (see Figure S1 in the Supporting Information). This indicates that independently of the metal/ligand ratio the oxidation of the metal occurs, leading to the formation of the bis-ligand complex.

The ¹H NMR spectrum of 1 at 25 °C in THF-*d*₈ (Figure S2, Supporting Information) displays nine paramagnetically shifted peaks and is consistent with the presence of D_{2h}-symmetric solution species, with three resonances for the four aromatic methyl and four amine methyl groups, two signals for the aromatic protons, and four signals for the two diastereotopic benzylic and the two diastereotopic methylenic bridge protons.

In order to probe the effect of bulky phenolate substituents in stabilizing a reduced species, the reaction between UI₃(THF)₄ and the more bulky ligand [K₂(salan-^tBu₂)], in a 1/1 ratio, was performed in different coordinating solvents (THF, CH₃CN, dme). In all the cases, the reaction led to the formation of a mixture of U(IV) species which were assigned from the NMR studies to the monoligand and bis-ligand complexes. The ¹H NMR spectra of the crude mixtures in toluene-*d*₈ at 25 °C display two distinct groups of resonances (Figure S3, Supporting Information): one group of narrow resonances, with a characteristic pattern of a C₂-symmetrical complex in solution, and one group of broad resonances. The first group was assigned to a mono-salan uranium(IV) complex. The broad resonances were attributed to the bis-ligand complex 2, and lowering the temperature of the sample in toluene-*d*₈ or THF-*d*₈ to −40 °C allowed the observation in the ¹H NMR spectrum of 4 resonances for the *tert*-butyl groups and 2 resonances for the methyl groups in the intensity ratio of 18/18/18/18/6/6 and 12 resonances with identical intensity (2H) that could be assigned to the methylenic and aromatic protons of the salan ligands of the complex [U(salan-^tBu₂)₂] (2).

Increasing the metal to ligand ratio to 1/2 enhanced the formation of the bis-ligand complex [U(salan-^tBu₂)₂] (2), which is the only species present in solution. Crystals of 2 suitable for X-ray diffraction analysis were grown by letting stand at room temperature a saturated acetonitrile solution (or tetrahydrofuran solution). Complex 2 can be obtained in 33% yield analytically pure from the reaction of UI₃(THF)₄ and K₂(salan-^tBu₂), in a 1/1 ratio.

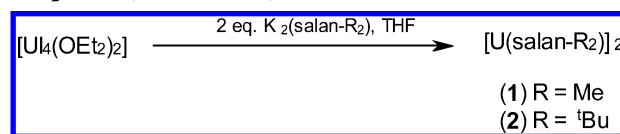
The salan uranium(IV) complexes 1 and 2 were probably formed by a disproportionation process promoted by the salan ligands, although the formation of U(0) metal could not be detected. An analogous behavior was reported by the Diaconescu group, showing that stoichiometric reactions between UI₃(THF)₄ and the dianionic ligands 2,6-bis(2,6-diisopropylanilidomethyl)pyridine (NN^{py})³¹ and ferrocene-diamide (NN^{fc})³⁰ give the complexes [U(NN^{py})₂], [U(NN^{py})₂], and [U(NN^{fc})I₂(THF)], respectively, in reproducible yields. The authors indicated that the uranium(IV) complexes were presumably formed by the disproportionation of uranium(III) intermediates to U(IV) and some form of U(0). This disproportionation pathway (U^{III} → U^{IV} + U⁰) has also been reported by other authors.^{58,59}

Disproportionation also occurs when the reaction of UI₃(THF)₄ with 1 equiv of [K₂(salan-^tBu₂)] is carried out in tetrahydrofuran in the presence of 2,2'-bipyridine. The proton NMR spectrum in toluene-*d*₈ of the reaction mixture at −40 °C shows the presence of two groups of NMR resonances, which were assigned to mono-ligand species and to the bis-ligand complex [U(salan-^tBu₂)₂] (2). Due to the similar solubilities of 2 and 3, it was not possible to isolate the bis-iodide 3 complex as an analytically pure compound. However, it was possible to isolate crystals suitable for X-ray diffraction analysis and confirm the structure of [U(salan-^tBu₂)(bipy)I₂] (3).

The ¹H NMR spectrum of 3 recorded in benzene-*d*₈ at 20 °C (Figure S4, Supporting Information) shows that the ONNO ligand protons feature an integration pattern consistent with an overall C₂-symmetric molecule in solution.

Uranium(IV) salan-R₂ Complexes. The homoleptic compounds [U(salan-R₂)₂] (R = Me (1), ^tBu (2)) can also be prepared in high yields by the salt-metathesis reactions between UI₄(L)₂ (L = Et₂O, PhCN) and 2 equiv of [K₂(salan-R₂)] in THF (Scheme 2).

Scheme 2. Synthesis of the Homoleptic [U(IV)(salan^{R2})₂] Complexes (R = Me, ^tBu)



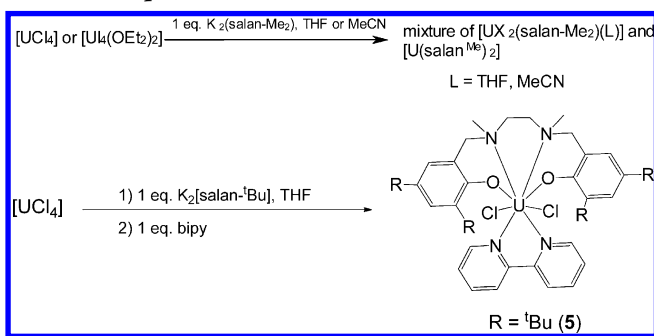
We have also investigated the possibility of preparing heteroleptic U(IV) complexes of salan-R₂ containing labile halide ligands, with the objective of identifying new precursors for the synthesis of U(IV) alkyl complexes.

The reaction of UI₄(Et₂O)₂ with K₂(salan-Me₂) in tetrahydrofuran, at room temperature, in a metal to ligand ratio of 1/1 (or less) always gave a mixture of the mono- and bis-ligand complexes (Figure S5, Supporting Information). The lower solubility of [U(salan-Me₂)I₂(CH₃CN)] (4) in comparison to 1 allowed the isolation of X-ray-quality crystals of 4 from a saturated acetonitrile solution of the reaction mixture. The proton NMR spectrum of crystals of 4 shows the presence

of C_2 -symmetric solution species (Figure S6, Supporting Information). However, the reproducible synthesis of complex **4** in an analytically pure form turned out to be difficult.

In order to identify synthetic routes to heteroleptic salan complexes suitable for reactivity studies, we have used UCl_4 as an alternative starting material for the preparation of these complexes. We expected that the chloride atoms would be less easily displaced during the salt-metathesis reactions, therefore leading to the stabilization of the mono-ligand complex. Nevertheless, in the case of the less bulky ligand (salan-Me_2) $^{2-}$ the reactions in a 1/1 ligand to metal ratio still gave a mixture of the mono-ligand and bis-ligand complexes (Figure S7, Supporting Information). To favor the formation of the bis-chloride complex, we then performed the reaction with the bulky $\text{K}_2(\text{salan-}^t\text{Bu}_2)$ ligand. The proton NMR in $\text{THF-}d_8$ at 25 °C of the reaction mixture of UCl_4 and 1 equiv of $\text{K}_2(\text{salan-}^t\text{Bu}_2)$ shows only one set of paramagnetically shifted resonances for the diamine bis(phenolate) ligand with an integration pattern consistent with a C_2 -symmetric compound in solution (Figure S8, Supporting Information). Several efforts were made to obtain crystals for X-ray diffraction analysis, but without success. However, the addition of 2,2'-bipyridine to a toluene solution of the isolated product led to the formation of $[\text{U}(\text{salan-}^t\text{Bu}_2)\text{Cl}_2(\text{bipy})]$ (**5**), confirming the formation of a monosubstituted species of the type $[\text{U}(\text{salan-}^t\text{Bu}_2)\text{Cl}_2(\text{THF})_x]$. Complex **5** was isolated in 61% yield by reacting UCl_4 with 1 equiv of $[\text{K}_2(\text{salan-}^t\text{Bu}_2)]$ in THF and in the presence of 2,2'-bipyridine (Scheme 3). Compound **5** is soluble in aromatic solvents and THF and insoluble in acetonitrile and *n*-hexane.

Scheme 3. Synthesis of the Heteroleptic U(IV) salan-R_2 /Halide Complexes



Crystal and Molecular Structures of the Uranium salan-R_2 Complexes. The molecular structures of the uranium salan complexes **2**–**5** were determined by single-crystal X-ray diffraction analysis.

The complex $[\text{U}(\text{salan-}^t\text{Bu}_2)_2]$ (**2**) crystallized from a THF solution as a tetrahydrofuran solvate and consists of discrete molecules in which the uranium(IV) center is eight-coordinated by two κ^4 -ONNO ligands (Figure 1). The coordination around the metal is best described as dodecahedral⁶⁰ with the two orthogonal trapezoids defined by the atoms $\text{O1}–\text{O1A}–\text{N2}–\text{N2A}$ and $\text{O2}–\text{O2A}–\text{N1}–\text{N1A}$ with a dihedral angle of 87.78(12)° between the two planes. The arrangement of the donor atoms around the uranium atom presents a crystallographically imposed C_2 symmetry that makes the two phenolate groups of the same diamine bis(phenolate) ligand identical and the two ONNO ligands different, which is consistent with the solution NMR data obtained at low temperature. The U–O

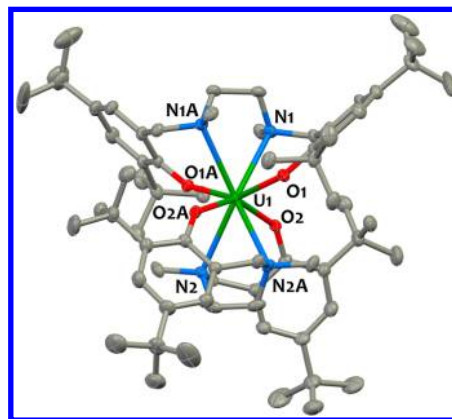


Figure 1. ORTEP view of the solid-state molecular structure of $[\text{U}(\text{salan-}^t\text{Bu}_2)_2]$ in 2·THF (50% probability ellipsoids). Hydrogen atoms and solvent molecules are omitted for clarity. Selected bond lengths (Å) and angles (deg): U–O(1) = 2.221(2), U–O(2) = 2.263(2), U–N(1) = 2.767(3), U–N(2) = 2.792(3); O(1)–U–O(1A) = 148.60(12), O(2)–U–O(2A) = 144.93(12), N(1)–U–N(1A) = 65.51(13), N(2)–U–N(2A) = 62.69(13).

bond distances of 2.219(2) and 2.263(2) Å are within the values reported for U(IV) phenolates.⁶¹ The U–N bond lengths of 2.790(2) and 2.766(2) Å are slightly longer than those found in the uranium(IV) bis(phenolate) complex $[\text{U}(\text{ONO}'\text{O})_2]$ (2.654(16) and 2.707(13) Å) ($\text{ONO}'\text{O} = \text{MeOCH}_2\text{CH}_2\text{N}(\text{CH}_2-(2-\text{O}-\text{C}_6\text{H}_2-\text{Bu}^t-3,5))_2$).⁶²

The complex $[\text{U}(\text{salan-}^t\text{Bu}_2)_2(\text{bipy})]$ (**3**) crystallized by slow diffusion of *n*-hexane into a saturated toluene solution with one independent molecule of **3** and two toluene molecules in the unit cell. The structure of **3** is shown in Figure 2 with selected bond lengths and angles.

The molecular structure shows that the uranium(IV) is eight-coordinated by the ONNO donors of the tetradentate $[\text{salan-}^t\text{Bu}_2]^{2-}$ ligand, by the two nitrogens of the bipyridine chelate, and by two iodine atoms. Although the arrangement of the donor atoms around the uranium atom in **3** results in the absence of crystallographic symmetry, the structure displays a

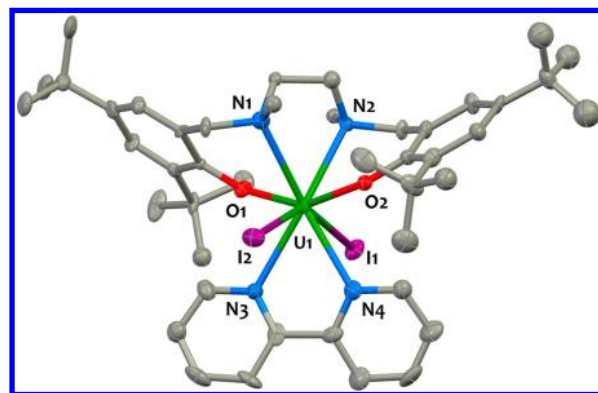


Figure 2. ORTEP view of the solid-state molecular structure of $[\text{U}(\text{salan-}^t\text{Bu}_2)_2\text{I}_2(\text{bipy})]$ (**3**) in 3·2 C_7H_8 (50% probability ellipsoids). Hydrogen atoms and solvent molecules are omitted for clarity. Selected bond lengths (Å) and angles (deg): U–O(1) = 2.128(8), U–O(2) = 2.118(8), U–N(1) = 2.705(9), U–N(2) = 2.702(9), U–N(3)(bipy) = 2.673(10), U–N(4)(bipy) = 2.663(10), U–I(1) = 3.2032(9), U–I(2) = 3.2020(9); O(1)–U–O(2) = 150.9(3), I(1)–U–I(2) = 142.83(3), N(1)–U–N(2) = 66.9(3), N(3)–U–N(4) = 61.2(3).

pseudo- C_2 axis that crosses the midpoint of the C–C bond linking the two pyridyl rings, which is consistent with the solution NMR data. The coordination geometry for the diiodide salan complex is irregular.

The U–O (2.118(8) and 2.128(8) Å) and U–N(salan) (2.704(9) and 2.702(9) Å) bond distances are slightly shorter than those found for compound **2**, certainly due to an increased steric congestion around the uranium center in complex **2** imposed by the coordination of two tetradentate salan ligands. The average U–N(bipy) bond distance of 2.668(15) Å is similar to U–N(bipy) bond distances reported for the U(IV) complexes $[\text{UCl}_4(\text{dmpe})(\text{Me}_2\text{bipy})]$ (dmpe = 1,2-bis-(dimethylphosphino)ethane; average 2.642(6) Å)⁶³ and $[\text{U}(\text{OSiMe}_3)_2\text{I}_2(\text{bipy})_2]$ (average 2.658(5) Å).⁶⁴ The C–C bond distance linking the two pyridyl rings of 1.515(18) Å is comparable with that of 1.490(3) Å in free bipyridine and in other reported bipyridine uranium complexes,^{65–67} confirming the C–C single-bond character. The bipyridine ligand is not planar, as expected for a neutral bipyridine upon coordination to a metal,⁶⁸ presenting a torsion angle between the two pyridyl rings of 17.9(8)°.

The complex $[\text{U}(\text{salan-Me}_2)_2\text{I}_2(\text{CH}_3\text{CN})]$ (**4**) crystallizes with one independent monomeric complex in the asymmetric unit. The molecular structure is presented in Figure 3.

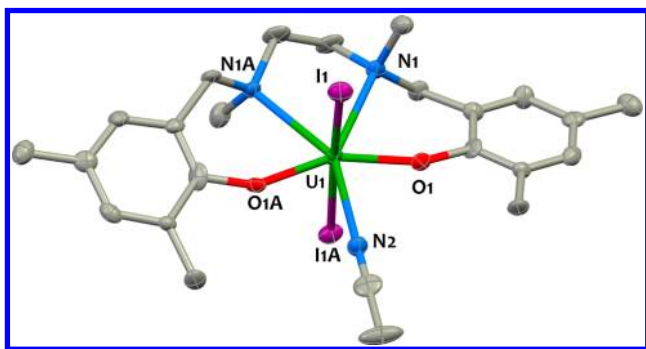


Figure 3. ORTEP view of the solid-state molecular structure of $[\text{U}(\text{salan-Me})_2\text{I}_2(\text{CH}_3\text{CN})]$ (**4**) (50% probability ellipsoids). Hydrogen atoms and solvent molecules are omitted for clarity. Selected bond lengths (Å) and angles (deg): U–O(1) = 2.078(5), U–N(1) = 2.700(5), U–N(2) = 2.591(7), U–I(1) = 3.0754(5); O(1)–U–O(1A) = 153.2(2), I(1)–U–I(1A) = 173.55(2), O(1)–U–N(2) = 76.58(12), O(1)–U–N(1) = 69.42(16), N(1)–U–N(1A) = 68.1(2), O(1)–U–I(1) = 91.46(12).

The structure shows that the metal is six-coordinated in a pentagonal-bipyramidal geometry, with the two iodide atoms occupying the apical positions of the bipyramid (I1–U–I1A = 173.55(2)°). The acetonitrile nitrogen atom and the ONNO-salan donors lie in the equatorial plane with X–M–X angles ranging between 68.1(2) and 76.58(12)°. The U–O (2.078(5) Å), U–N(salan) (2.700(5) Å), and U–I bond lengths (3.0754(5) Å) are shorter than those observed for **2** and **3**, as expected for a less sterically crowded complex with a lower coordination number.

The complex $[\text{U}(\text{salan-}^t\text{Bu}_2)_2\text{Cl}_2(\text{bipy})]$ (**5**) crystallized by slow diffusion of *n*-hexane into a saturated toluene solution with one toluene molecule in the asymmetric unit. The X-ray diffraction structure shows that compound **5** is isomorphous with **3** (Figure 4), with a pseudo- C_2 axis crossing the C–C bond linking the two pyridyl rings of the bipyridine. As observed for the diiodide uranium salan complex, the

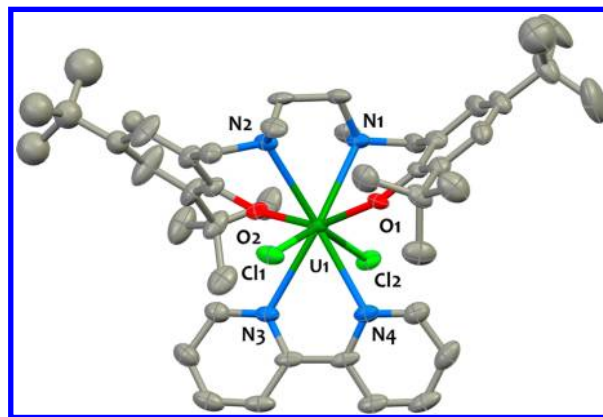


Figure 4. ORTEP view of the solid-state molecular structure of $[\text{U}(\text{salan-}^t\text{Bu}_2)_2\text{Cl}_2(\text{bipy})]$ (**5**) (50% probability ellipsoids; one of the *t*Bu groups could not be refined anisotropically). Hydrogen atoms and solvent molecules are omitted for clarity. Selected bond lengths (Å) and angles (deg): U–O(1) = 2.163(3), U–O(2) = 2.151(3), U–N(1) = 2.702(4), U–N(2) = 2.674(4), U–N(3)(bipy) = 2.677(4), U–N(4)(bipy) = 2.677(4), U–Cl(1) = 2.7356(11), U–Cl(2) = 2.6985(12); O(1)–U–O(2) = 151.63(12), Cl(1)–U–Cl(2) = 144.37(4), N(1)–U–N(2) = 67.58(12), N(3)–U–N(4) = 61.07(14).

coordination sphere around the uranium center is highly distorted.

The average U–O, U–N, and U–N(bipy) bond distances are almost identical with those found for complex **3**. The average U–Cl bond lengths of 2.717(1) Å in **5** is within the values for other uranium(IV) chlorides reported in the literature (2.617(3)–2.719(1) Å).^{69,70} The C–C bond distance linking the two pyridyl rings of 1.466(8) Å and the torsion angle between the two pyridyl rings of 15.9(3)° are also characteristic of the coordination of a neutral bipyridine ligand to the uranium center.

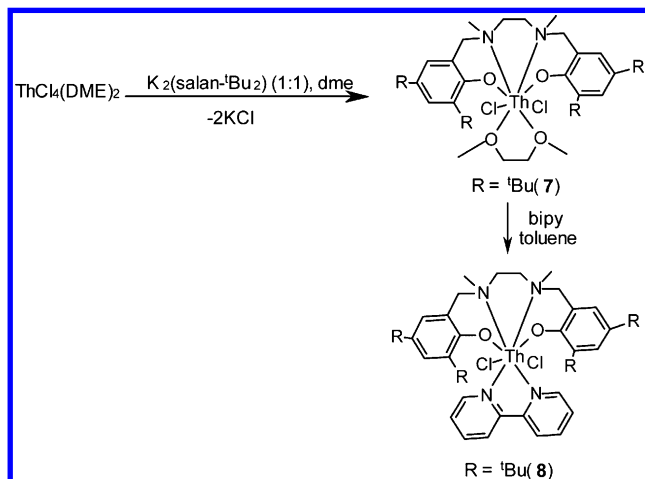
Thorium(IV) salan- R_2 Complexes. On the basis of the information obtained with uranium, we have also investigated the possibility of preparing analogous thorium(IV) salan complexes.

The reaction of $\text{ThCl}_4(\text{dme})_2$ with $\text{K}_2(\text{salan-}^t\text{Bu}_2)$ in tetrahydrofuran, at room temperature, in a metal to ligand ratio of 1/2 gave a mixture of the mono- and bis-ligand complexes. It was not possible to isolate the complex $[\text{Th}(\text{salan-}^t\text{Bu}_2)_2]$ (**6**) in an analytically pure form. Only a few crystals suitable for X-ray diffraction analysis were obtained from a saturated *n*-hexane solution, which allowed us to confirm the presence in the reaction mixture of the bis-ligand thorium complex **6**.

As depicted in Scheme 4, the reaction of $\text{ThCl}_4(\text{dme})_2$ with 1 equiv of $\text{K}_2(\text{salan-}^t\text{Bu}_2)$ in dme, at room temperature, afforded the monosubstituted thorium complex $[\text{Th}(\text{salan-}^t\text{Bu})\text{Cl}_2(\text{dme})]$ (**7**) as a white solid in good yield.

The thorium diamine bis(phenolate) complex **7** was fully characterized by ESI/MS and ^1H and ^{13}C NMR spectroscopy. The ^1H NMR spectra of **7** in benzene- d_6 , at room temperature, display chemical shifts in the range of 0–8 ppm with well-resolved coupling patterns, consistent with a diamagnetic compound and also reflecting the presence of C_2 -symmetric complexes in solution, as observed for the dihalide uranium-(IV) salan complexes. The ancillary ligand displays one set of resonances for the phenolate groups and one resonance for the methylene protons, while the diastereotopic methylenic bridge protons appear as two doublets and the diastereotopic benzylic

Scheme 4. Synthesis of Mono-salan Thorium(IV) Chloride Complexes



protons appear as a typical AB discrete doublet at 5.24 and 2.77 ppm. The difference in chemical shifts observed for the diastereotopic benzyl protons is remarkable and more pronounced than those observed for salan-transition-metal complexes.^{53,71} An analogous observation was reported for the amine bis(phenolate) complex $[\text{Th}(\text{ONOO})\text{Cl}_2]$ ($\text{ONOO} = \text{MeOCH}_2\text{CH}_2\text{N}(\text{CH}_2-(2-\text{O}-\text{C}_6\text{H}_2-\text{Bu}^t_{2-3,5}))_2$),⁷² indicating that one set of the benzylic protons is closer to the electropositive metal center. The signals corresponding to the methylene groups of the coordinated dme in $[\text{Th}(\text{salan-}^t\text{Bu}_2)\text{Cl}_2(\text{dme})]$ (7) are very broad. Decreasing the temperature of the NMR sample to -10°C , in toluene- d_8 , allowed the observation of two doublets at 3.76 and 2.65 ppm for the diastereotopic CH_2 protons of the symmetrically coordinated dme molecule. The C_2 symmetry in solution was also confirmed by the ^{13}C NMR data. Although the NMR data and the other analyses were consistent with the formulation proposed, the solid-state structures of the dme adduct could not be determined.

^1H NMR studies in benzene- d_6 showed that the coordinated dme molecule in 7 is quantitatively replaced by the 2,2'-bipyridine chelate. The same reaction carried out in toluene (Scheme 4) led to the isolation of the complex $[\text{Th}(\text{salan-}^t\text{Bu}_2)\text{Cl}_2(\text{bipy})]$ (8) as a white solid in 79% yield. The ^1H NMR spectrum of 8 is consistent with an overall C_2 -symmetric structure in solution, in agreement with the pseudo- C_2 symmetry found in the solid state for 8 (see below). The ^{13}C NMR spectra confirmed all the conclusions drawn from ^1H NMR spectral analysis. The proton and carbon chemical shift assignments for compounds 7 and 8 were made on the basis of ^1H - ^1H COSY and ^1H - ^{13}C HSQC experiments.

Crystal and Molecular Structures of the Thorium salan Complexes. The complex $[\text{Th}(\text{salan-}^t\text{Bu}_2)_2]$ (6) crystallizes in the monoclinic space group $\text{C}2/c$ as an n -hexane solvate and is isostructural with $[\text{U}(\text{salan-}^t\text{Bu}_2)_2]$ (2) (Figure 5). Complex 6 exhibits a distorted-dodecahedral geometry, in which the two orthogonal trapezoids are defined by $\text{O}2-\text{O}2\text{A}-\text{N}1-\text{N}1\text{A}$ and $\text{O}1-\text{O}1\text{A}-\text{N}2-\text{N}2\text{A}$ with a dihedral angle of $87.85(5)^\circ$. As observed for the uranium complex, the thorium(IV) complex presents a crystallographically imposed C_2 symmetry, which is consistent with the solution NMR data. The $\text{Th}-\text{O}$ (2.276(2) and 2.295(2) Å) and $\text{Th}-\text{N}$ (2.807(2) and 2.819(2) Å) bond lengths are slightly longer than the corresponding distances observed for the uranium bis-

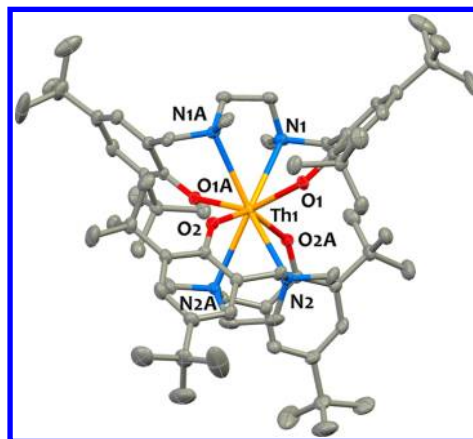


Figure 5. ORTEP view of the solid-state molecular structure of $[\text{Th}(\text{salan-}^t\text{Bu}_2)_2]$ (6) (50% probability ellipsoids) in $6 \cdot \text{C}_6\text{H}_{14}$. Hydrogen atoms and solvent molecules are omitted for clarity. Selected bond lengths (Å) and angles (deg): $\text{Th}-\text{O}(1) = 2.2755(18)$, $\text{Th}-\text{O}(2) = 2.2950(15)$, $\text{Th}-\text{N}(1) = 2.8194(19)$, $\text{Th}-\text{N}(2) = 2.807(2)$; $\text{O}(1)-\text{Th}-\text{O}(1\text{A}) = 147.03(8)$, $\text{O}(2)-\text{Th}-\text{O}(2\text{A}) = 144.37(8)$, $\text{N}(1)-\text{Th}-\text{N}(1\text{A}) = 60.17(8)$, $\text{N}(2)-\text{Th}-\text{N}(2\text{A}) = 62.38(9)$.

(salan- $^t\text{Bu}_2$) complex 2, which can be explained by the larger ionic radius of $\text{Th}(\text{IV})$.⁷³ The mean value of the $\text{Th}-\text{O}$ bond distance (2.285(2) Å) is similar to that found in the amine bis(phenolate) complex $[\text{Th}(\text{ONOO})_2]$ (2.266(4) Å).⁷²

Crystals suitable for X-ray diffraction analysis were obtained in the case of $[\text{Th}(\text{salan-}^t\text{Bu}_2)\text{Cl}_2(\text{bipy})]$ (8) by slow diffusion of n -hexane into a saturated toluene solution. Complex 8 crystallizes in the trigonal space group $\text{R}\bar{3}$ as a toluene solvate. The arrangement of the donor atoms around the thorium atom in 8 results in a crystallographic C_1 symmetry but approximates a C_2 symmetry; small variations of the angles in solution could be enough to result in a symmetrical compound in solution, as observed by NMR analysis.

Compound 8 is isomorphous with the uranium complex 5 (Figure 6) and, as expected, has an identical molecular structure

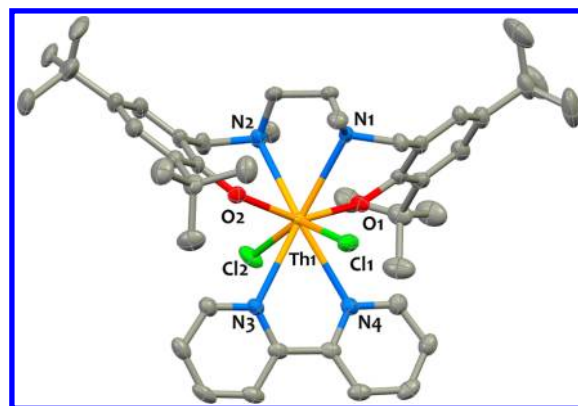
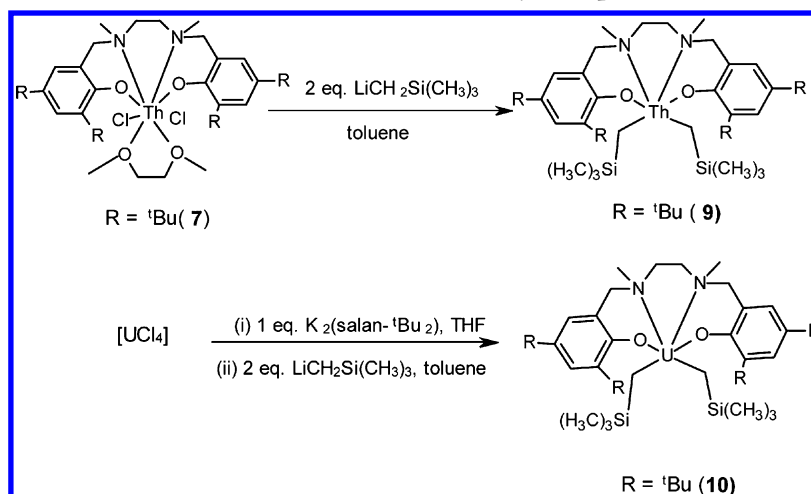


Figure 6. ORTEP view of the solid-state molecular structure of $[\text{Th}(\text{salan-}^t\text{Bu}_2)\text{Cl}_2(\text{bipy})]$ (8) in $8 \cdot 1.5\text{C}_7\text{H}_8$ (50% probability ellipsoids). Hydrogen atoms and solvent molecules are omitted for clarity. Selected bond lengths (Å) and angles (deg): $\text{Th}-\text{O}(1) = 2.227(3)$, $\text{Th}-\text{O}(2) = 2.225(3)$, $\text{Th}-\text{N}(1) = 2.748(4)$, $\text{Th}-\text{N}(2) = 2.707(4)$, $\text{Th}-\text{N}(3)(\text{bipy}) = 2.717(4)$, $\text{Th}-\text{N}(4)(\text{bipy}) = 2.724(4)$, $\text{Th}-\text{Cl}(1) = 2.7647(11)$, $\text{Th}-\text{Cl}(2) = 2.7342(12)$; $\text{O}(1)-\text{Th}-\text{O}(2) = 150.03(11)$, $\text{Cl}(1)-\text{Th}-\text{Cl}(2) = 145.54(4)$, $\text{N}(1)-\text{Th}-\text{N}(2) = 66.30(11)$, $\text{N}(3)-\text{Th}-\text{N}(4) = 59.42(11)$.

Scheme 5. Synthesis of Mono-salan Thorium(IV) and Uranium(IV) Alkyl Complexes



and very similar bond distances and angles. The bond distances, with differences of 0.07 Å for M–O, 0.04 Å for M–N(salan), 0.04 Å for M–N(bipy), and 0.05 Å for M–Cl, are in line with the 0.05 Å difference in ionic radii for U(IV) and Th(IV).⁷³ The average thorium–oxygen bond length is 2.228(6) Å and compares well with the value of 2.266(4) Å found in the eight-coordinate amine bis(phenolate) complex Th(ONOO)₂.⁷² The pyridyl rings of the bipyridine ligand are twisted with respect to each other, with a torsion angle of 8.3(2)°. The value of the bond distance (1.486(8) Å) for the C–C linking the two pyridyl rings is nearly identical with those found in the free bipyridine and in the recently structurally characterized complex $[\{\eta^5\text{-}1,2,4\text{-(Me}_3\text{C)C}_5\text{H}_2\}\text{Th(SePh)}_3(\text{bipy})]$ (1.484(9) Å)⁷⁴ and is longer than the value found for the thorium complex $[\{\eta^5\text{-}1,2,4\text{-(Me}_3\text{C)C}_5\text{H}_2\}_2\text{Th(bipy)}]$ ⁷⁴ (1.382(8) Å) with a dianionic bipyridine ligand. The average Th–N(bipy) bond distance in **8** (2.720(6) Å) is much longer than the value found in the cyclopentadienyl thorium complex with anionic bipyridine (2.344(5) Å), as expected, and slightly longer than the average Th–N bond distance (2.609(5) Å) in the cyclopentadienyl complex with neutral bipyridine.

Thorium(IV) and Uranium(IV) Alkyl Derivatives. The reaction of $[\text{Th(salan-}^1\text{Bu}_2)\text{Cl}_2(\text{dme})]$ (**7**) with 2 equiv of LiCH₂SiMe₃ in toluene at room temperature led to the formation of the Th(IV) dialkyl complex $[\text{Th(salan-}^1\text{Bu}_2)(\text{CH}_2\text{SiMe}_3)_2]$ (**9**) (Scheme 5).

The dialkyl complex was obtained as a white crystalline solid in 89% yield. Single crystals of $[\text{Th(salan-}^1\text{Bu}_2)(\text{CH}_2\text{SiMe}_3)_2]$ (**9**) crystallizing in the centrosymmetric monoclinic *C*2/*c* space group were grown by slow evaporation of a toluene/*n*-hexane solution. The thorium center is hexacoordinated (Figure 7) and adopts a distorted-octahedral geometry, in which the phenolate oxygens are mutually trans with an O–Th–O angle of 154.57(10)°, as observed for group 4 salan complexes.⁵³ The alkyl groups are *cis*, as well as the amine nitrogen atoms of the ancillary ligand, with C–Th–C and N–Th–N angles of 111.34(15) and 64.67(11)°, respectively.

Consistent with the solution NMR data, the two alkyl groups are symmetrical, as the structure possesses an imposed crystallographic *C*₂ axis, and the Th–C bond distance of 2.529(3) Å is comparable to those reported for the bis(trimethylsilylmethyl) complexes $[(\text{XA}_2)\text{ThR}_2]$ (*H*₂–XA₂ = 4,5-bis(2,6-diisopropylanilino)-2,7-di-*tert*-butyl-9,9-dimethyl-xanthene) (2.476(6) Å),³⁴ $[\{\text{Me}_2\text{Si(C}_5\text{Me}_4)_2\}\text{ThR}_2]$ (2.52(2)

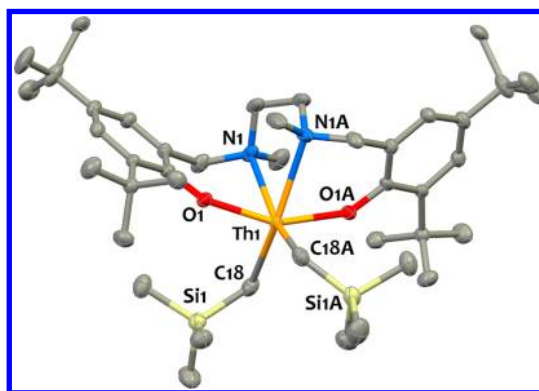


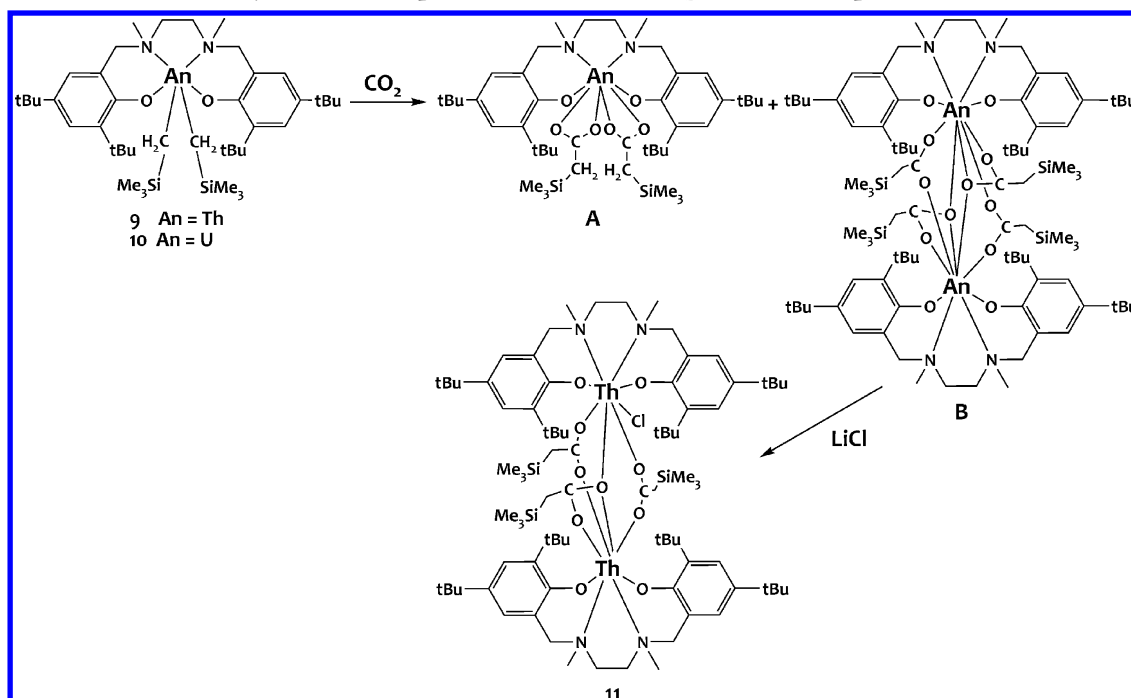
Figure 7. ORTEP view of the solid-state molecular structure of $[\text{Th(salan-}^1\text{Bu}_2)(\text{CH}_2\text{SiMe}_3)_2]$ (**9**) (50% probability ellipsoids). Hydrogen atoms are omitted for clarity. Selected bond lengths (Å) and angles (deg): Th–O(1) = 2.202(2), Th–N(1) = 2.706(2), Th–C(18) = 2.529(3); O(1)–Th–O(1A) = 154.57(10), C(18)–Th–N(1A) = 155.16(10), Th–C(18)–Si(1) = 118.3(1), C(18)–Th–N(1) = 92.61(9), N(1)–Th–N(1A) = 64.17(11), C(18)–Th–C(18A) = 111.34(15).

Å),⁷⁵ $[(2,6\text{-}^1\text{Bu}_2\text{H}_3\text{C}_6\text{O})_2\text{ThR}_2]$ (2.46(2) Å),²⁷ $[\text{Cp}^*(2,6\text{-}^1\text{Bu}_2\text{H}_3\text{C}_6\text{O})\text{ThR}_2]$ (2.474 Å),⁷⁶ and $[(^i\text{Pr}_2\text{PhNCOCN})\text{Th}(\text{CH}_2\text{SiMe}_3)_2]$ (2.50(1) Å).⁷⁷

The Th–N bond length of 2.706(2) Å and the Th–O bond distance of 2.202(2) Å are shorter than those in complex **8**, due to the lower coordination number. The Th–C–Si angle in **9** is 118.29(1)°, which is close to the angle expected for a *sp*³-hybridized carbon atom.

Structurally characterized thorium dialkyl complexes supported by noncarbocyclic ligands are rare,^{27,32,34,77} and to the best of our knowledge, **9** represents the first structurally characterized dialkyl actinide complex supported by a dianionic tetradentate ligand.

The ¹H and ¹³C NMR data (Figures S9 and S10, Supporting Information) of **9** corroborate the formation of the dialkyl complex, and as found for the other thorium complexes, one set of resonances is observed for the diamine bis(phenolate) ligand, consistent with a *C*₂-symmetric molecular structure in solution. As a result of the ligand coordination, the benzylic and methylenic protons are diastereotopic, giving rise to one ¹H AB spin system and two doublets, respectively. The Th–CH₂ resonances give rise to two doublets at 0.30 and 0 ppm with

Scheme 6. Reaction of the Dialkyl An(IV) Complexes with 1 atm of CO₂ at Room Temperature

²J(H,H) = 10.2 Hz in the ¹H NMR and one signal at 87.2 ppm in the carbon spectrum. The chemical shifts are in conformity with other thorium bis(trimethylsilylmethyl) complexes reported.^{27,32,34,75,77} The ¹H and ¹³C resonances of **9** were assigned with the support of ¹H–¹H COSY and ¹H–¹³C HSQC spectra.

The analogous complex [U(salan-^tBu₂)(CH₂SiMe₃)₂] (**10**) was synthesized by reacting [U(salan-^tBu₂)Cl₂(thf)_x], prepared in situ from the reaction of UCl₄ with 1 equiv of [K₂(salan-^tBu₂)] in tetrahydrofuran, with 2 equiv of LiCH₂SiMe₃ in toluene (Scheme 5). Crystals of **10** were obtained by slow evaporation of an *n*-hexane solution. The X-ray diffraction analysis showed that the uranium bis(alkyl) is isostructural⁷⁸ with **9**. However, the crystallographic data were not of very good quality, and therefore the structure will not be discussed in detail. Nevertheless, the structure possesses enough quality to indicate atom connectivity, showing that the uranium(IV) center is six-coordinated by the κ⁴-ONNO salan ligand and by two trimethylsilylmethyl groups.

The ¹H NMR spectrum of **10** is paramagnetically shifted, and the resonances were assigned on the basis of the signal integration (Figure S11, Supporting Information) is consistent with a C₂-symmetric molecular structure in solution. The diastereotopic U–CH₂ protons are significantly upfield at –236.4 and –238.5 ppm, probably due to the close proximity of the CH₂ protons to the paramagnetic center.

Both An–dialkyl complexes are stable at room temperature for several weeks in benzene-*d*₆ or toluene-*d*₈ solution but decompose 50% and 25% for [Th(salan-^tBu₂)(CH₂SiMe₃)₂] (**9**) and [U(salan-^tBu₂)(CH₂SiMe₃)₂] (**10**), respectively, over 9 h at 70 °C in toluene-*d*₈. The small differences found in the stabilities of **9** and **10** probably result from the different degrees of steric saturation of the coordination spheres of these actinide metals. Higher stabilities have been reported for thorium alkyls of highly rigid dianionic bidentate noncarbocyclic ligands,³⁴ but the stability of complexes **9** and **10** is comparable to the thermal stability reported for actinide(IV) cyclopentadienyl

dialkyl complexes.^{75–77,79} and for dialkyl complexes of Th(IV) containing monoanionic monodentate *tert*-butylphenoxides as ancillary ligands.²⁷

Reactivity of An–Bis(alkyl) Complexes with CO₂

Insertion of small molecules into metal–carbon bonds is an important step in many metal-mediated chemical transformations. Carbon dioxide insertion into metal–carbon bonds has been extensively explored for transition metals and lanthanides and yields carboxylates.^{80–85} The insertion of CO₂ into an actinide–carbon bond has been observed in the presence of carbocyclic ancillary ligands,^{4,22,23,41,86–89} the first example being reported by Marks and Moloy in 1985,²³ but is more rare and only four examples of structurally characterized insertion products have been reported.^{20,22,41,89} Preliminary experiments on the reaction of the [An(salan-^tBu₂)(CH₂SiMe₃)₂] complexes (An = Th (**9**), U (**10**)) with CO₂ were carried out on an NMR scale and followed by ¹H NMR and ESI/MS. Treatment of a toluene-*d*₈ solution of **9** with excess CO₂ at room temperature, over 1 h, led to disappearance of the ¹H NMR resonances corresponding to the bis(alkyl) species **9** and the emergence of broad resonances in a very simple spectrum (Figure S12-a, Supporting Information), where the Si(CH₃)₃ protons appear as a broad singlet at 0.81 ppm and the aromatic protons of the salan-^tBu phenolate groups appear as two broad signals at 7.48 and 6.89 ppm. When the sample temperature was lowered, it was possible to observe at –50 °C the split of the resonance at 0.81 ppm into various singlets with different integrations (Figure S12-b, Supporting Information). However, the identification and assignment of the ¹H NMR spectrum proved to be difficult due to signal overlapping. The NMR analysis indicates that the reaction [Th(salan-^tBu₂)(CH₂SiMe₃)₂]/excess CO₂ produces complex product mixtures, which might be involved in fluxional behavior.

Treating the thorium bis(alkyl) complex with 2 equiv of CO₂ led to the observation of ¹H NMR spectra, at 20 °C and at low temperature, with profiles similar to those observed in the

reaction with excess CO_2 . The ^{13}C NMR at 20 °C also presented broad resonances (Figure S13, Supporting Information), but it was possible to observe resonances at 190.3 and -1.26 ppm that could be attributed to carboxylate⁹⁰ and $\text{Si}(\text{CH}_3)_3$ carbon resonances, respectively. The complexity of the NMR spectra indicates the presence of an equilibrium between different products or isomers in solution, which could result from different coordination modes of the CO_2 fragment (Scheme 6).⁹¹

The ESI/MS analysis of the CO_2 reactions (Figure S14, Supporting Information), in the positive ion mode, showed two peaks at m/z 1039.9 and 2056.1 corresponding to $[\text{Th}(\text{salan-}^t\text{Bu}_2)(\text{O}_2\text{CCH}_2\text{SiMe}_3)_2\text{Na}]^+$ and $[\{\text{Th}(\text{salan-}^t\text{Bu}_2)(\text{O}_2\text{CCH}_2\text{SiMe}_3)_2\}_2\text{Na}]^+$ (the sodium cation is present in the electrospray source), respectively, and in the negative ion mode one peak at m/z 1051.9 corresponding to $[\text{Th}(\text{salan-}^t\text{Bu}_2)(\text{O}_2\text{CCH}_2\text{SiMe}_3)_2\text{Cl}]^-$. These results are consistent with the formation of monomeric and dimeric insertion products of CO_2 into the two Th–C bonds. The ESI/MS studies also indicated that the CO_2 insertion occurred into the Th–C(alkyl) bond and not into the Th–salan ligand bonds, as collision-induced dissociation (CID) experiments with $[\text{Th}(\text{salan-}^t\text{Bu}_2)(\text{O}_2\text{CCH}_2\text{SiMe}_3)_2\text{Na}]^+$ showed elimination of neutral sodium carboxylate $[\text{NaO}_2\text{CCH}_2\text{SiMe}_3]$ (Figure S15, Supporting Information).

Several attempts were made to obtain crystals of a bis- CO_2 insertion thorium compound. In one of these attempts, a few colorless crystals were obtained by slow evaporation of a toluene solution of the $[\text{Th}(\text{salan-}^t\text{Bu}_2)(\text{CH}_2\text{SiMe}_3)_2]/\text{CO}_2$ reaction mixture, which were identified as the dimeric complex $[\text{Th}_2\text{Cl}(\text{salan-}^t\text{Bu}_2)_2(\mu\text{-}\eta^1\text{:}\eta^1\text{-O}_2\text{CCH}_2\text{SiMe}_3)_2(\mu\text{-}\eta^1\text{:}\eta^2\text{-O}_2\text{CCH}_2\text{SiMe}_3)]$ (**11**) by X-ray diffraction analysis. The ORTEP diagram and selected bond lengths and angles are depicted in Figure 8.

Complex **11** contains two thorium centers bridged by two symmetrical $\mu\text{-}\eta^1\text{:}\eta^1$ and one unsymmetrical $\mu\text{-}\eta^1\text{:}\eta^2$ carboxylato ligands. The Th...Th distance is 4.7536(3) Å. Each thorium atom is eight-coordinated, however, with different coordination spheres. One thorium atom is coordinated by the two symmetrically bridging carboxylato oxygen atoms, by two η^2 oxygen atoms of the unsymmetrically bridging $\mu\text{-}\eta^1\text{:}\eta^2$ carboxylato ligand, and by the tetradentate salan ligand. The other thorium atom is coordinated by two $\mu\text{-}\eta^1\text{:}\eta^1$ bridging carboxylato oxygen atoms, by one oxygen atom of the $\mu\text{-}\eta^1\text{:}\eta^2$ carboxylato ligand, by one chloride atom, and by the tetradentate ONNO chelate. The coordination geometry around the two thorium centers is described as a distorted dodecahedron, where the two nearly orthogonal trapezoids for Th(1) (88.2(1)°) are defined by N1–N2–O2–O5 and O1–O10–O9–O7, with deviations from planarity of 8.2(2) and 13.8(2)°, and for Th(2) (88.7(1)°) defined by N3–N4–O8–O3 and O4–Cl1–O9–O6.

The Th–N and Th–O(Ar) distances are similar to those found for **6** and **8**. However, the O(Ph)–Th–O(Ph) angles of 104.9(2) and 98.3(1)° are significantly smaller than those found for **6** and **8**, which present values close to 150°. This indicates that the salan- $^t\text{Bu}_2$ ligand adopts a different conformation in the dimeric complex **11**, demonstrating its flexibility and ability to adapt to diverse metal environments.

The average Th–O bond lengths (2.406(3) Å) of the bridging (bidentate) carboxylato ligand are in agreement with previously reported Th–O bond lengths involving $\eta^1\text{:}\eta^1$ bridging carboxylato ligands.^{92,93} The Th–O bond lengths of

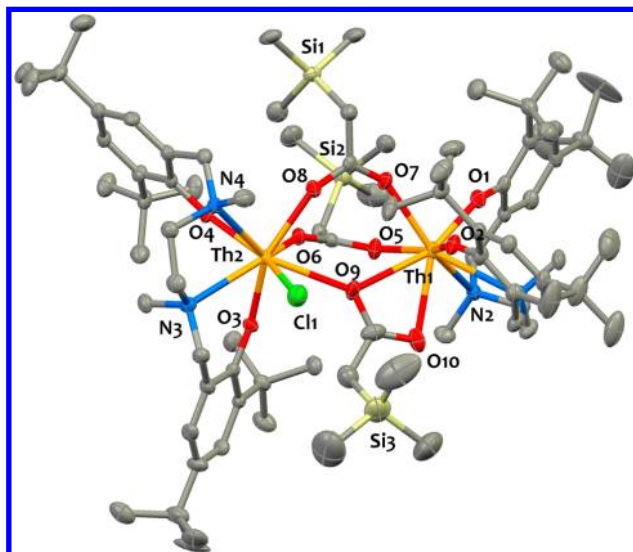


Figure 8. ORTEP view of the solid-state molecular structure of $[\text{Th}_2\text{Cl}(\text{salan-}^t\text{Bu}_2)_2(\mu\text{-}\eta^1\text{:}\eta^1\text{-O}_2\text{CCH}_2\text{SiMe}_3)_2(\mu\text{-}\eta^1\text{:}\eta^2\text{-O}_2\text{CCH}_2\text{SiMe}_3)]$ (**11**) (50% probability ellipsoids). Hydrogen atoms and solvent molecules are omitted for clarity. Selected bond lengths (Å) and angles (deg): Th(1)–O(1) = 2.200(3), Th(1)–O(2) = 2.196(3), Th(2)–O(3) = 2.198(3), Th(2)–O(4) = 2.213(3), Th(1)–N(1) = 2.778(4), Th(1)–N(2) = 2.757(4), Th(2)–N(3) = 2.751(4), Th(2)–N(4) = 2.813(4), Th(1)–O(5) = 2.379(3), Th(1)–O(7) = 2.407(3), Th(1)–O(9) = 2.611(3), Th(1)–O(10) = 2.552(4); O(1)–Th–O(2) = 104.94(12), O(3)–Th–O(4) = 98.29(11), average O–C–O(carboxylato) = 123.35(75), N(1)–Th(1)–N(2) = 65.85(11), N(3)–Th(2)–N(4) = 65.43(11), O(9)–C–O(10) = 123.8(5).

the $\mu\text{-}\eta^1\text{:}\eta^2$ carboxylato ligand are longer, ranging from 2.552(4) to 2.611(3) Å, and are comparable with the average value found in the complex $[\text{Th}(\text{HIDA})_2(\text{C}_2\text{O}_4)]$ (2.59(3) Å; H_2IDA = iminodiacetic) containing a bidentate chelate carboxylato group.⁹³ The similar values of the O–C bond lengths (1.262(6) and 1.259(7) Å; 1.252(7) and 1.276(5) Å; 1.305(8) and 1.334(8) Å) indicate delocalization of an electron over the O–C–O group in the three fragments.

While the structure of the product of the insertion of CO_2 into a Th(IV)–arene bond has been reported,⁸⁹ complex **11** is, to the best of our knowledge, the first example of a crystallographically characterized thorium(IV) carboxylate complex prepared by insertion reaction of carbon dioxide into a Th–C(alkyl) bond.

The structure of **11** shows that CO_2 insertion into the Th–C(alkyl) bonds occurred, with one thorium atom coordinated to three carboxylato ligands and the other thorium atom coordinated to three bridging carboxylates and one chloride. The presence of the coordinated chloride ligand is ascribed to the presence of small amounts of LiCl in the sample of complex **9** reacted with CO_2 . Attempt to obtain crystals from the reaction of higher purity samples of **9** with CO_2 have failed so far. The ESI/MS analysis of the reaction mixture $[\text{Th}(\text{salan-}^t\text{Bu}_2)(\text{CH}_2\text{SiMe}_3)_2]/\text{CO}_2$ after addition of excess LiCl (Figure S16, Supporting Information) showed a significant increase of the peak at m/z 955.9, corresponding to $[\text{Th}(\text{salan-}^t\text{Bu})(\text{O}_2\text{CCH}_2\text{SiMe}_3)_2\text{Cl}]^-$, and a decrease of the peak corresponding to $[\text{Th}(\text{salan-}^t\text{Bu})(\text{O}_2\text{CCH}_2\text{SiMe}_3)_2\text{Cl}]^-$ (m/z 1051.9), indicating that a carboxylate ligand is easily replaced by a chloride. A complex with four bridging carboxylates is sterically crowded, and the presence of LiCl in the solution facilitates the displacement of a carboxylate ligand

by a small ligand, such as the chloride. Removal of carboxylate by a chloride ligand after CO₂ insertion into the metal–carbon bond has been previously reported and could be used to complete a cycle by regenerating the halide precursor.^{20,41,94}

When an analogous reaction with 2 equiv of CO₂ was performed with the uranium bis(alkyl) **10**, the reaction proved to be slower. After 1 h at room temperature, the ¹H NMR spectrum still displayed resonances of the starting complex **10**, and several new resonances appeared. A group of relatively sharp resonances with six distinguishable resonances, integrating for 9 protons each (Figure S17, Supporting Information), was observed and assigned to four ^tBu groups, one SiMe₃ of the alkyl ligand, and one SiMe₃ group of a carboxylato ligand. This is consistent with the existence in solution of a reduced-symmetry system, which could be attributed to the formation of an intermediate mono-CO₂ insertion product of the type “[U(salan-^tBu₂)(O₂CCH₂SiMe₃)(CH₂SiMe₃)]”. Additionally, the observation of two resonances strongly shifted upfield (−221.80 and −233.52 ppm) and typically assigned to U–CH₂ protons also supports this interpretation. After 18 h of reaction, the signals assigned to the mono-CO₂ insertion product disappeared (Figure S19, Supporting Information). The proton NMR after 18 h shows two sets of signals for which the most intense peaks could be clearly identified. One set of signals consists of two resonances at 47.23 (18H) and 10.28 ppm (18H), one resonance at −71.80 ppm (6H), and one resonance at −12.439 ppm (18H), which could be assigned to the ^tBu groups of the aromatic phenolates, to the NMe₃ groups, and to the SiMe₃ groups of the carboxylato ligands, respectively. This is consistent with the presence of a high-symmetry species, with the chemical shifts of the ^tBu groups falling in the same spectral region as those observed for the other C₂-symmetric monomeric uranium compounds described in this work. These observations led us to assign these signals to a monomeric compound of the type [U(salan-^tBu₂)(O₂CCH₂SiMe₃)₂] (complex A in Scheme 6), presenting the same coordination mode for the two carboxylate ligands. The second sets of signals of resonances present six resonances of equal intensity, which could be assigned to four ^tBu groups and two carboxylate ligands in a dimeric compound containing two carboxylate ligands with different coordination modes, as observed for the thorium CO₂ insertion product **11**. However, an X-ray diffraction structure is required to confirm the nuclearity and coordination mode of the carboxylate ligand in these species. The presence of other signals on the spectrum, corresponding probably to other minor species and some decomposition products which could arise from the loss of carboxylate ligands, rendered difficult the full assignment of the ¹H NMR spectrum and the isolation of an analytically pure product. The high solubility of the [U(salan-^tBu₂)(CH₂SiMe₃)₂]/CO₂ reaction mixture has so far prevented the isolation of single crystals adequate for X-ray diffraction analysis.

The ESI/MS analysis results (Figure S20, Supporting Information) are in agreement with the formation of monomeric and dimeric bis-CO₂ insertion products. CID experiments with [U(salan-^tBu₂)(O₂CCH₂SiMe₃)₂Na]⁺ also showed elimination of neutral sodium carboxylate [NaO₂CCH₂SiMe₃] (Figure S21, Supporting Information), as observed for the case of thorium, confirming that the CO₂ insertion occurred into the U–C(alkyl) bonds.

CONCLUSIONS

The ability of tetradentate salan-R₂^{2−} (R = Me, ^tBu) to act as a supporting ligand in low-valent uranium chemistry has been explored. The salan ligands did not allow the synthesis of stable complexes of U(III), and the reaction of U(III) with K₂salan-R₂ induced disproportionation to U(IV) and U(0), affording mixtures of bis-ligand and monoligand complexes.

Stable mononuclear homoleptic bis-ligand complexes of U(IV) can be prepared in good yield by salt metathesis by reacting U(IV) halides with the K₂salan-R₂ ligands independently of the ligand bulk (R = Me, ^tBu). In contrast, mononuclear heteroleptic complexes of the formula [An(salan-^tBu₂)Cl₂] can only be isolated in pure form for the bulky salan-^tBu₂ ligand. The reactions of U(IV) and Th(IV) halides with K₂salan-Me₂ always afford a mixture of mono- and bis-ligand complexes independently of the metal to ligand ratios, due to the high stability of the bis-ligand complexes. These results show that the ligand substituents can be used to favor the formation of the targeted compound in these salan systems. The halide complexes [An(salan-^tBu₂)Cl₂] provide versatile precursors for the synthesis of stable dialkyl complexes.

Preliminary studies show that CO₂ inserts rapidly into the An(IV)–C(alkyl) bond after reaction of the salan-^tBu₂-supported dialkyl complexes at room temperature with 1 atm of CO₂, leading to multiple insertion products. The structure of the insertion product isolated for thorium shows that insertion of CO₂ occurs in both alkyl groups and that the resulting carboxylate is easily displaced by a chloride anion, probably as a result of the important steric bulk of the salan-^tBu₂ ligand.

Finally, we have demonstrated that salan ligands provide a new example of effective supporting ligands in organoactinide chemistry. Future studies will be directed to investigate the influence of the ligand architecture on the structure and reactivity of dialkyl complexes of actinide(IV) using aminephenolate ligands with different substituents and with more rigid amine scaffolds.

ASSOCIATED CONTENT

Supporting Information

CIF files giving complete crystallographic data for the crystal structures of **2–6**, **8**, **9**, and **11** and figures giving ¹H NMR spectra for compounds **2–5**, **9**, and **10**, and NMR and ESI-MS spectra of the An–bis(alkyl) reactions with CO₂. This material is available free of charge via the Internet at <http://pubs.acs.org>.

AUTHOR INFORMATION

Corresponding Author

*M.M.: tel, (+33)438783955; fax, (+33)438785090; e-mail, marinella.mazzanti@cea.fr. L.M.: tel, (+351) 21-994 6197; e-mail, leonorm@itn.pt.

Notes

The authors declare no competing financial interest.

ACKNOWLEDGMENTS

E.M., L.M., I.C.S., A.C., J.M.C., and J.M. are grateful to the Fundação para a Ciência e a Tecnologia (FCT) for funding: research project PTDC/QUI/66187/2006, RNEM-Rede Nacional de Espectrometria de Massa/ITN Node (REDE/1503/REM/2005), and “Ciência 2008” Programme. B.B., C.C., J.P., and M.M. acknowledge support from the Commissariat à l’Energie Atomique, Direction de l’Energie Nucléaire, RBPCH program and by the “Agence Nationale de la Recherche”

(ANR-10-BLAN-0729). This work also benefited from COST Action CM1006-EUFEN: European F-Element Network.

REFERENCES

- (1) Andrea, T.; Eisen, M. S. *Chem. Soc. Rev.* **2008**, 37, 550.
- (2) Fox, A. R.; Bart, S. C.; Meyer, K.; Cummins, C. C. *Nature* **2008**, 455, 341.
- (3) Castro-Rodriguez, I.; Nakai, H.; Zakharov, L. N.; Rheingold, A. L.; Meyer, K. *Science* **2004**, 305, 1757.
- (4) Lam, O. P.; Meyer, K. *Polyhedron* **2012**, 32, 1.
- (5) Diaconescu, P. L.; Arnold, P. L.; Baker, T. A.; Mindiola, D. J.; Cummins, C. C. *J. Am. Chem. Soc.* **2000**, 122, 6108.
- (6) Arnold, P. L.; Turner, Z. R.; Bellabarba, R. M.; Tooze, R. P. *Chem. Sci.* **2011**, 2, 77.
- (7) Camp, C.; Mougél, V.; Horeglad, P.; Pecaut, J.; Mazzanti, M. *J. Am. Chem. Soc.* **2010**, 132, 17374.
- (8) Barnea, E.; Eisen, M. S. *Coord. Chem. Rev.* **2006**, 250, 855.
- (9) Stubbert, B. D.; Stern, C. L.; Marks, T. J. *Organometallics* **2003**, 22, 4836.
- (10) Barnea, E.; Andrea, T.; Berthet, J. C.; Ephritikhine, M.; Eisen, M. S. *Organometallics* **2008**, 27, 3103.
- (11) Barnea, E.; Andrea, T.; Kapon, M.; Berthet, J. C.; Ephritikhine, M.; Eisen, M. S. *J. Am. Chem. Soc.* **2004**, 126, 10860.
- (12) Ephritikhine, M. *New J. Chem.* **1992**, 16, 451.
- (13) Bruno, J. W.; Stecher, H. A.; Morss, L. R.; Sonnenberger, D. C.; Marks, T. J. *J. Am. Chem. Soc.* **1986**, 108, 7275.
- (14) Marks, T. J.; Seyam, A. M. *J. Am. Chem. Soc.* **1972**, 94, 6545.
- (15) Marks, T. J.; Seyam, A. M.; Kolb, J. R. *J. Am. Chem. Soc.* **1973**, 95, 5529.
- (16) Pool, J. A.; Scott, B. L.; Kiplinger, J. L. *J. Am. Chem. Soc.* **2005**, 127, 1338.
- (17) Pool, J. A.; Scott, B. L.; Kiplinger, J. L. *Chem. Commun.* **2005**, 2591.
- (18) Siladke, N. A.; Ziller, J. W.; Evans, W. J. *J. Am. Chem. Soc.* **2011**, 133, 3507.
- (19) Evans, W. J.; Walensky, J. R.; Furche, F.; Ziller, J. W.; DiPasquale, A. G.; Rheingold, A. L. *Inorg. Chem.* **2008**, 47, 10169.
- (20) Webster, C. L.; Ziller, J. W.; Evans, W. J. *Organometallics* **2012**, 31, 7191–7197.
- (21) Evans, W. J.; Walensky, J. R.; Ziller, J. W. *Organometallics* **2010**, 29, 945.
- (22) Evans, W. J.; Walensky, J. R.; Ziller, J. W. *Inorg. Chem.* **2010**, 49, 1743.
- (23) Moloy, K. G.; Marks, T. J. *Inorg. Chim. Acta* **1985**, 110, 127.
- (24) Jantunen, K. C.; Burns, C. J.; Castro-Rodriguez, I.; Da Re, R. E.; Golden, J. T.; Morris, D. E.; Scott, B. L.; Taw, F. L.; Kiplinger, J. L. *Organometallics* **2004**, 23, 4682.
- (25) Stubbert, B. D.; Marks, T. J. *J. Am. Chem. Soc.* **2007**, 129, 4253.
- (26) Fortier, S.; Melot, B. C.; Wu, G.; Hayton, T. W. *J. Am. Chem. Soc.* **2009**, 131, 15512.
- (27) Clark, D. L.; Grumbine, S. K.; Scott, B. L.; Watkin, J. G. *Organometallics* **1996**, 15, 949.
- (28) Turner, H. W.; Andersen, R. A.; Zalkin, A.; Templeton, D. H. *Inorg. Chem.* **1979**, 18, 1221.
- (29) Domingos, A.; Marques, N.; Dematos, A. P.; Santos, I.; Silva, M. *Organometallics* **1994**, 13, 654.
- (30) Duhovic, S.; Khan, S.; Diaconescu, P. L. *Chem. Commun.* **2010**, 46, 3390.
- (31) Monreal, M. J.; Diaconescu, P. L. *Organometallics* **2008**, 27, 1702.
- (32) Jantunen, K. C.; Batchelor, R. J.; Leznoff, D. B. *Organometallics* **2004**, 23, 2186.
- (33) Jantunen, K. C.; Haftbaradaran, F.; Katz, M. J.; Batchelor, R. J.; Schatte, G.; Leznoff, D. B. *Dalton Trans.* **2005**, 3083.
- (34) Cruz, C. A.; Emslie, D. J. H.; Harrington, L. E.; Britten, J. F.; Robertson, C. M. *Organometallics* **2007**, 26, 692.
- (35) Cruz, C. A.; Emslie, D. J. H.; Jenkins, H. A.; Britten, J. F. *Dalton Trans.* **2010**, 39, 6626.
- (36) Monreal, M. J.; Diaconescu, P. L. *J. Am. Chem. Soc.* **2010**, 132, 7676.
- (37) Monreal, M. J.; Khan, S.; Diaconescu, P. L. *Angew. Chem., Int. Ed.* **2009**, 48, 8352.
- (38) Broderick, E. M.; Gutzwiller, N. P.; Diaconescu, P. L. *Organometallics* **2010**, 29, 3242.
- (39) Hayes, C. E.; Platel, R. H.; Schafer, L. L.; Leznoff, D. B. *Organometallics* **2012**, 31, 6732.
- (40) Hayes, C. E.; Leznoff, D. B. *Organometallics* **2010**, 29, 767.
- (41) Matson, E. M.; Forrest, W. P.; Fanwick, P. E.; Bart, S. C. *J. Am. Chem. Soc.* **2011**, 133, 4948.
- (42) Cohen, A.; Yeori, A.; Kopilov, J.; Goldberg, I.; Kol, M. *Chem. Commun.* **2008**, 2149.
- (43) Yeori, A.; Goldberg, I.; Shuster, M.; Kol, M. *J. Am. Chem. Soc.* **2006**, 128, 13062.
- (44) Liu, X. L.; Shang, X. M.; Tang, T.; Hu, N. H.; Pei, F. K.; Cui, D. M.; Chen, X. S.; Jing, X. B. *Organometallics* **2007**, 26, 2747.
- (45) Horeglad, P.; Nocton, G.; Filinchuk, Y.; Pecaut, J.; Mazzanti, M. *Chem. Commun.* **2009**, 1843.
- (46) Nocton, G.; Horeglad, P.; Vetere, V.; Pecaut, J.; Dubois, L.; Maldivi, P.; Edelstein, N. M.; Mazzanti, M. *J. Am. Chem. Soc.* **2010**, 132, 495.
- (47) Vetere, V.; Maldivi, P.; Mazzanti, M. *C. R. Chim.* **2010**, 13, 876.
- (48) Clark, D. L.; Sattelberger, A. P.; Andersen, R. A. *Inorg. Synth.* **1997**, 31, 307.
- (49) Sun, Y.; McDonald, R.; Takats, J.; Day, V. W.; Eperspacher, T. A. *Inorg. Chem.* **1994**, 33, 4433.
- (50) Hermann, J. A.; Suttle, J. F. *Inorg. Synth.* **1957**, 5, 143.
- (51) Cantat, T.; Scott, B. L.; Kiplinger, J. L. *Chem. Commun.* **2010**, 46, 919.
- (52) Enriquez, A. E.; Scott, B. L.; Neu, M. P. *Inorg. Chem.* **2005**, 44, 7403.
- (53) Tshuva, E. Y.; Goldberg, I.; Kol, M. *J. Am. Chem. Soc.* **2000**, 122, 10706.
- (54) SADABS and ABSPACK: Area-Detector Absorption Correction; Siemens Industrial Automation, Madison, WI, 1996.
- (55) Sheldrick, G. M. *SHELXS-97*, 6.14 ed.; University of Göttingen, Göttingen, Germany, 2006.
- (56) Altomare, A.; Burla, M. C.; Camalli, M.; Cascarano, G. L.; Giacovazzo, C.; Guagliardi, A.; Moliterni, A. G. G.; Polidori, G.; Spagna, R. *J. Appl. Crystallogr.* **1999**, 32, 115.
- (57) Farrugia, L. J. *J. Appl. Crystallogr.* **2012**, 45, 849.
- (58) Odom, A. L.; Arnold, P. L.; Cummins, C. C. *J. Am. Chem. Soc.* **1998**, 120, 5836.
- (59) Lewis, A. J.; Williams, U. J.; Kikkawa, J. M.; Carroll, P. J.; Schelter, E. J. *Inorg. Chem.* **2012**, 51, 37.
- (60) Muetterties, E. L.; Guggenberger, L. J. *J. Am. Chem. Soc.* **1974**, 96, 1748.
- (61) Vandersluys, W. G.; Sattelberger, A. P. *Chem. Rev.* **1990**, 90, 1027.
- (62) Drew, M. G. B. *Coord. Chem. Rev.* **1977**, 24, 179.
- (63) Newell, B. S.; Schwaab, T. C.; Shores, M. P. *Inorg. Chem.* **2011**, 50, 12108.
- (64) Brown, J. L.; Mokhtarzadeh, C. C.; Lever, J. M.; Wu, G.; Hayton, T. W. *Inorg. Chem.* **2011**, 50, 5105.
- (65) Antunes, M. A.; Pereira, L. C. J.; Santos, I. C.; Mazzanti, M.; Marcalo, J.; Almeida, M. *Inorg. Chem.* **2011**, 50, 9915.
- (66) Maria, L.; Domingos, A.; Galvao, A.; Ascenso, J.; Santos, I. *Inorg. Chem.* **2004**, 43, 6426.
- (67) Mehdoui, T.; Berthet, J. C.; Thuery, P.; Salmon, L.; Riviere, E.; Ephritikhine, M. *Chem. Eur. J.* **2005**, 11, 6994.
- (68) Schultz, M.; Boncella, J. M.; Berg, D. J.; Tilley, T. D.; Andersen, R. A. *Organometallics* **2002**, 21, 460.
- (69) Cantat, T.; Scott, B. L.; Morris, D. E.; Kiplinger, J. L. *Inorg. Chem.* **2009**, 48, 2114.
- (70) Thomson, R. K.; Graves, C. R.; Scott, B. L.; Kiplinger, J. L. *Inorg. Chim. Acta* **2011**, 369, 270.

- (71) (a) Shimrit Gendler, S.; Segal, S.; Goldberg, I.; Goldschmidt, Z.; Kol, M. *Inorg. Chem.* **2006**, *45*, 4783–4790. (b) Balsells, J.; Carroll, P. J.; Walsh, P. J. *Inorg. Chem.* **2001**, *40*, 5568–5574.
- (72) Andrea, T.; Barnea, E.; Botoshansky, M.; Kapon, M.; Genizi, E.; Goldschmidt, Z.; Eisen, M. S. *J. Organomet. Chem.* **2007**, *692*, 1074.
- (73) Shannon, R. D. *Acta Crystallogr. Sect. A* **1976**, *32*, 751.
- (74) Ren, W. S.; Zi, G. F.; Walter, M. D. *Organometallics* **2012**, *31*, 672.
- (75) Bruno, J. W.; Smith, G. M.; Marks, T. J.; Fair, C. K.; Schultz, A. J.; Williams, J. M. *J. Am. Chem. Soc.* **1986**, *108*, 40.
- (76) Butcher, R. J.; Clark, D. L.; Grumbine, S. K.; Scott, B. L.; Watkin, J. G. *Organometallics* **1996**, *15*, 1488.
- (77) Hayes, C. H.; Platel, R. H.; Schafer, L. L.; Leznoff, D. B. *Organometallics* **2012**, *31*, 6732.
- (78) Crystal data for $[\text{U}(\text{salan-}^t\text{Bu}_2)(\text{CH}_2\text{SiMe}_3)_2]$ (**10**): monoclinic, space group *Cc*, $a = 20.1132(8)$ Å, $b = 10.3705(4)$ Å, $c = 21.8851(9)$ Å, $\beta = 92.249(1)^\circ$, $V = 4565.31(5)$ Å³.
- (79) Fendrick, C. M.; Schertz, L. D.; Day, V. W.; Marks, T. J. *Organometallics* **1988**, *7*, 1828.
- (80) Correa, A.; Martin, R. *Angew. Chem., Int. Ed.* **2009**, *48*, 6201.
- (81) Darensbourg, D. J.; Kudarowski, R. A. *Adv. Organomet. Chem.* **1983**, *22*, 129.
- (82) Zhou, X. G.; Zhu, M. *J. Organomet. Chem.* **2002**, *647*, 28.
- (83) Evans, W. J.; Rego, D. B.; Ziller, J. W.; DiPasquale, A. G.; Rheingold, A. L. *Organometallics* **2007**, *26*, 4737.
- (84) Evans, W. J.; Miller, K. A.; Ziller, J. W. *Inorg. Chem.* **2006**, *45*, 424.
- (85) Liu, R. T.; Zhou, X. G. *J. Organomet. Chem.* **2007**, *692*, 4424.
- (86) Evans, W. J.; Walensky, J. R.; Ziller, J. W. *Organometallics* **2010**, *29*, 945.
- (87) Evans, W. J.; Siladke, N. A.; Ziller, J. W. *C. R. Chim.* **2010**, *13*, 775.
- (88) Trnka, T. M.; Bonanno, J. B.; Bridgewater, B. M.; Parkin, G. *Organometallics* **2001**, *20*, 3255.
- (89) Korobkov, I.; Gambarotta, S. *Organometallics* **2004**, *23*, 5379.
- (90) Nakajima, Y.; Okuda, J. *Organometallics* **2007**, *26*, 1270.
- (91) Evans, W. J.; Brady, J. C.; Ziller, J. W. *J. Am. Chem. Soc.* **2001**, *123*, 7711.
- (92) Ok, K. M.; Sung, J.; Hu, G.; Jacobs, R. M. J.; O'Hare, D. *J. Am. Chem. Soc.* **2008**, *130*, 3762.
- (93) Thuery, P. *Inorg. Chem.* **2011**, *50*, 1898.
- (94) Gardner, B. M.; Stewart, J. C.; Davis, A. L.; McMaster, J.; Lewis, W.; Blake, A. J.; Liddle, S. T. *Proc. Natl. Acad. Sci. U.S.A.* **2012**, *109*, 9265.